Ph. D. DISSERTATION

HIGHLY EFFICIENT AND STABLE HYBRID WHITE ORGANIC LIGHT-EMITTNG DIODES BASED ON THE MIXED HOST SYSTEM

혼합물 호스트 발광층 기반 고효율 장수명
하이브리드 백색 유기 발광 다이오드

BY

YONGWON KWON

FEBRUARY 2017

DEPARTMENT OF
ELECTRICAL AND COMPUTER ENGINEERING
COLLEGE OF ENGINEERING
SEOUL NATIONAL UNIVERSITY

HIGHLY EFFICIENT AND STABLE HYBRID WHITE ORGANIC LIGHT-EMITTING DIODES BASED ON THE MIXED HOST EMITTING LAYER SYSTEM

혼합물 호스트 발광층 기반 고효율 장수명 하이브리드 백색 유기 발광 다이오드

지도교수 이 창 희

이 논문을 공학박사 학위논문으로 제출함

2017 년 2 월

서울대학교 대학원

전기컴퓨터공학부

권 용 원

권용원의 공학박사 학위논문을 인준함

2017 년 2 월

위 원 장 : _____ (인)
부위원장 : _____ (인)
위 원 : _____ (인)
위 원 : _____ (인)
위 원 : _____ (인)

Abstract

HIGHLY EFFICIENT AND STABLE HYBRID WHITE ORGANIC LIGHT-EMITTING DIODES BASED ON THE MIXED HOST EMITTING LAYER SYSTEM

YONGWON KWON

DEPARTMENT OF ELECTRICAL AND COMPUTER ENGINEERING
COLLEGE OF ENGINEERING

SEOUL NATIONAL UNIVERSITY

In this thesis, we have investigated the design strategy of high-performance hybrid white organic-light emitting diodes (WOLEDs) and degradation mechanism of blue OLEDs based on thermally activated delayed fluorescent (TADF) emitter by using mixed host system. First, we demonstrated the high-performance hybrid WOLEDs with general fluorescent blue emitter having non-interlayer structure. The major feature of developed device is exciton manipulation using mixed host in blue

emitting layer (EML). The developed non-interlayer hybrid WOLED exhibited enhanced performance compared to interlayer structure device and we investigated the electroluminescence (EL) process of non-interlayer device. However, non-interlayer device in this thesis has poor lifetime compared to that of interlayer device and it was due to the inevitable mutual exciton quenching between long wavelength phosphor and blue fluorophore which has low lying triplet energy level. From these results, we clearly see the necessity of blue fluorescent material having high triplet energy level. Thus, we adopted thermally activated fluorescent (TADF) emitter.

Next, we investigated the degradation mechanisms of blue OLEDs based on TADF emitter and demonstrated that mixed host system can improve device stability. The main cause of degradation of OLEDs with TADF blue emitter was the host instability. Additionally, the electrochemical instability of molecules influences long-term OLED degradation. Also the formation of exciton quenchers and non-radiative recombination centers acts to reduce OLED luminance. The mixed host can be easily utilized and improve the device lifetime by enhancing stability on excited-state stress.

Finally, we have investigated high-performance hybrid WOLEDs with superior efficiency, color stability, low efficiency roll-off, and device stability based on blue TADF emitter with mixed host. The resulting WOLED shows the maximum external quantum efficiency, current efficiency, and power efficiency of 22.1 %, 59.3 cd/A, and 50.3 lm/W, respectively. Moreover, the device exhibits extremely stable EL spectra with Commision Internationale de L'Eclairage (CIE) coordinates of (0.417, 0.422). We also characterized the exciton generation zone in the EML with versatile experimental and theoretical evidences. In addition, the investigated hybrid WOLED based on TADF emitter exhibited 2 times enhanced device lifetime compared to the device without mixed host system.

In conclusion, the mixed host system has successfully utilized for achieving high-performance hybrid WOLEDs and stable blue OLEDs based on TADF emitter. The mixed host effectively broadens the exciton generation zone and improves the stability on excited-state stress. The investigated mechanisms and optimization procedure reported in this thesis can be anticipated as starting point for further research towards high performance stable hybrid WOLEDs.

Keywords: Organic Light-Emitting Diodes, Hybrid White, Thermally Activated Delayed Fluorescence, Lifetime

Student Number: 2013-30219

Contents

Abstract i

Contents iv

List of Figures viii

List of Tables xiii

Chapter 1 1

1.1 Organic Light-Emitting Diodes **1**

1.2 White Organic Light-Emitting Diodes **6**

1.3 Outline of Thesis **10**

Chapter 2 **11**

2.1 Materials **11**

2.1.1 Preparation of Organic Materials **11**

2.1.2 Chemical structures of Organic Materials **11**

2.2 Device Fabrication and Characterization Methods **14**

2.2.1 Device Fabrication Methods **14**

2.2.2 Current-Voltage-Luminance Measurement **15**

2.2.3 Efficiency Calculation Methods **19**

2.2.4 Transient Electroluminescence Measurement **20**

2.2.5 Other Characterization Methods **21**

Chapter 3 **22**

3.1 The determination of interlayer composition for efficient hybrid WOLEDs **25**

3.2 Non-interlayer hybrid WOLEDs using mixed host for blue EML **32**

3.3 Influence of blue EML host structure to white device stability **41**

3.4 Summary **44**

Chapter 4 **45**

4.1 The effect of mixed host structure on blue OLEDs based on TADF emitter.....47

4.2 Degradation mechanisms of TADF based blue OLEDs53

4.3 Appendix.....61

4.4 Summary.....62

Chapter 5 **63**

5.1 Hybrid white OLEDs based on TADF blue emitter without mixed host system.....65

5.2 The stability issues in TADF based hybrid WOLEDs .73

5.3 Hybrid white OLEDs based on TADF blue emitter with mixed host system.....74

5.4 The stability of hybrid WOLEDs with mixed host.....84

5.5 Summary.....86

Chapter 6 **87**

Bibilography **89**

Publication **101**

List of Figures

Figure 1.1 Various application products of OLEDs. Samsung mobile display, LG TV display, LG Chemical solid state lighting, LG Display flexible display (clockwise) 2

Figure 1.2 Efficiency improvement of WOLEDs over past 20 years. The red box exhibits the results without outcoupling technique. 7

Figure 2.1 Chemical structures of di-[4-(N,N-ditolyl-amino)-phenyl]cyclohexane (TAPC), 4,4',4''-tris(carbazol-9-yl)triphenylamine (TCTA), and 1,3-bis(carbazol-9-yl)benzene (mCP) as hole transporting materials and host materials. 12

Figure 2.2 Chemical structures of bis[2-(diphenylphosphino)phenyl]ether oxide (DPEPO), and 1,3,5-tri[(3-pyridyl)-phen-3-yl]benzene (TmPyPB) as electron transporting materials and host materials. 12

Figure 2.3 Chemical structures of 9-(9-phenylcarbazole-3-yl)-10-(naphthalene-1-yl)anthracene (PCAN), bis[4-(9,9-dinethyl-9,10-dihydroacridine)phenyl]sulfone (DMAC-DPS) as blue emitters, iridium(III)bis(4-phenylthieno[3,2-c]pyridinato-N,C2') acetylacetonate (PO-01), and iridium(III)bis(4-(4-*t*-butylphenyl)thieno[3,2-*c*]pyridinato-*N*,*C*2')acetylacetonate ($Ir(tptpy)_2(acac)$) as yellow emitters. 13

Figure 2.4 Schematic diagrams for the measurement of (a) I-V-L characteristics and (b) EL spectra. 16
Figure 2.5 (a) The CIE standard observer color-matching functions and (b) the CIE 1931 color space chromaticity diagram. The outer boundary is the spectral locus, with wavelengths shown in nanometers. 18
Figure 2.6 The set-up for the transient electroluminescence (T-EL) measurement...20
Figure 3.1 Exciton energy diagram and energy transfer mechanisms possible in electroluminescence (EL) process of hybrid WOLEDs with interlayer 26
Figure 3.2 The structure of EML proposed on this study.....27
Figure 3.3 Electroluminescence spectra of hybrid OLEDs with various blend interlayers, measured at 5.1 mA/cm^2. The influence of the interlayer blend is visible.....28
Figure 3.4 External quantum efficiencies of the two-color hybrid white OLEDs. The efficiencies are dependent on the spectrum. 29
Figure 3.5 The current density-voltage characteristics of (a) hole-only devices of yellow emitters, (b) electron-only devices of yellow emitters, (c) hole-only devices of blue emitters, and (d) electron-only devices of blue emitters. The hole only device structure: ITO/MoO_3 (10 nm)/TCTA (20 nm)/EML (30 nm)/TCTA (20 nm)/MoO_3 (10 nm)/Al. The electron only device structure: Al/LiF (1 nm)/TmPyPB (20 nm)/EML (30 nm)/TmPyPB (20 nm)/LiF (1 nm)/Al 31
Figure 3.6 Energy level scheme for EML used in the hybrid white OLED, The red box with dotted line exhibits exciton generation zone 32
Figure 3.7 (a) Current density-voltage-luminance characteristics and (b) external quantum efficiency and power efficiency versus current density characteristics 35

Figure 3.8 The normalized EL spectra at different current density levels of (a) interlayer structure, and (b) non-interlayer structure hybrid WOLEDs.36

Figure 3.9 (a) External quantum efficiency and power efficiency versus current density characteristics, (b) normalized EL spectra of white device with TmPyPB as blue emitting layer host. (c) and (d) show those of white device with TCTA as host.....38

Figure 3.10 The normalized EL spectra for (a) device A with structure of ITO/TAPC/TCTA (5 nm)/$(ppy)_2$Ir(acac) (0.1 nm)/TCTA (5 nm)/TCTA:TmPyPB:PCAN (2:1, 4 %, 8 nm)/TmPyPB (30 nm)/LiF/Al and (b) device B with structure of ITO/TAPC/TCTA (10 nm)/TCTA:TmPyPB:PCAN (2:1, 4 %, 8 nm)/TmPyPB (5 nm)/$(ppy)_2$Ir(acac) (0.1 nm)/TmPyPB (25 nm)/LiF/Al. 40

Figure 3.11 Transient EL decay profile measured at 560 nm of the devices with and without PCAN doping. 41

Figure 3.12 (a) The lifetime of fabricated devices, and (b) the external quantum efficiency versus current density characteristics. The inset shows the normalized EL spectra 43

Figure 4.1 (a) Chemical structures of the DMAC-DPS, mCP, and DPEPO and energy level diagram of (b) TADF based OLEDs, (c) HODs, and (d) EODs. 48

Figure 4.2 (a) Current density versus voltage (J-V) characteristics and (b) luminance versus voltage (L-V) of TADF based blue OLEDs. 50

Figure 4.3 (a) External quantum efficiency with respect to current density, (b) the luminance degradation of TADF based blue OLEDs. 51

Figure 4.4 Summarized device parameters of (a) driving voltage at 500 cd/m^2 and LT50, and (b) EQE at 500 cd/m^2 and critical current density J_c.....52

Figure 4.5 Changes in PL/PL_0 of the EML composite films as a function of operational time. 54
Figure 4.6 Changes in PL/PL_0 of (a) HODs, and (b) EODs under continuous constant-current bias as a function of operational time. 55
Figure 4.7 Changes in V/V_0 of (a) HODs, and (b) EODs under constant-current bias as a function of operational time. 56
Figure 4.8 Summarized changes in L/L0 of the OLEDs and PL/PL0 of the composite films, EODs, and HODs of (a) device with mCP:DPEPO 1:1 as host, and (b) DPEPO as host. 58
Figure 4.9 Transient EL decay curves of fabricated blue TADF OLEDs with different host structures. 60
Figure 4.10 The optical microscopy images of fabricated pixels. 61
Figure 5.1 The energy level diagram of emitting layer of hybrid WOLED. Solid lines and dashed lines refer to HOMO and LUMO energy levels. Circles and triangles correspond to the exciton energies. 65
Figure 5.2 (a) Current density-voltage-luminance characteristics of white device, and (b) external quantum efficiency and power efficiency versus luminance characteristics of white device. The inset represents the normalized EL spectra at different driving current density. 68
Figure 5.3 Time-resolved EL decay curves of (a) white device measured at 460 nm wavelength, and (b) white device and device without DMAC-DPS measured at 560 nm wavelength. 70
Figure 5.4 (a) Normalized EL spectra, and (b) EQE and PE versus luminance of white devices with different yellow phosphor doping concentration. ...72
Figure 5.5 (a) The lifetime of WOLED in this section, and (b) normalized EL spectrum change with degradation. 73

Figure 5.6 The schematic diagram of emitting layer of fabricate device in this section. Circles show single exciton energy level and triangles show triplet exciton energy level. 74

Figure 5.7 (a) Current density-voltage (J-V) characteristics and (b) luminance-voltage (L-V) characteristics of fabricated hybrid WOLEDs.....77

Figure 5.8 (a) External quantum efficiency and (b) power efficiency versus luminance of fabricated hybrid WOLEDs.....78

Figure 5.9 The normalized EL spectra of (a) device A, (b) device B, and (c) device C with respect to the different current density. 80

Figure 5.10 The transient EL decay curves of fabricated WOLEDs based on mixed host. 82

Figure 5.11 The transient EL decay curves of the devices with and without DMAC-DPS.....82

Figure 5.12 (a) Device lifetime curves and (b) EQE versus luminance of fabricated WOLEDs. The device without mixed host system exhibited short device lifetime and large efficiency roll-off.....85

List of Tables

Table 1.1 The status of emitting materials for OLEDs.....5

Table 3.1 The various device characteristics of hybrid white OLEDs with respect to interlayer composition. 29

Table 3.2 Comparison of the device performances of the previously reported hybrid WOLEDs a: single-EML, b: multi-EML.....34

Table 4.1 Summary of the parameters of TADF blue OLEDs with mixed host. 52

Table 4.2 Summarized parameters of transient EL decay curves of fabricated blue TADF OLEDs with different host structures. 59

Table 5.1 Comparison of the device performances for the representative WOLEDs. 67

Table 5.2 Summary of the performance of fabricated white devices. *Critical current density, where EQE declines by half from its maximum, **driving current density from 2.55 mA/cm^2 to 25.5 mA/cm^2. 75

Table 5.3 Summary of fitted parameters for transient decay curves. 83

Table 5.4 Summary of efficiency roll-off and device lifetime trends. 83

Chapter 1

Introduction

1.1 Organic Light-Emitting Diodes

Organic light-emitting diodes (OLEDs) have attracted a great attention due to their application in full-color displays and solid-state lighting sources and now lead Korean display industry. The OLEDs have superior advantages such as thin, light, high efficiency, vivid color, and availability for flexible device, and potential for low-cost fabrication.

Recently, full-color OLEDs display have commercialized on mobile and TV applications. Samsung mass-produced high resolution flexible mobile display for their premium smartphone galaxy S7 series and LG produced flagship smart TVs using white OLEDs combined with color filters. Also, some solid-state lighting sources using OLEDs are on market. LG Chemical installed the OLED lighting sources is Seoul National University central library, which exhibited their technical potential. Figure 1.1 shows the representative OLED based products.

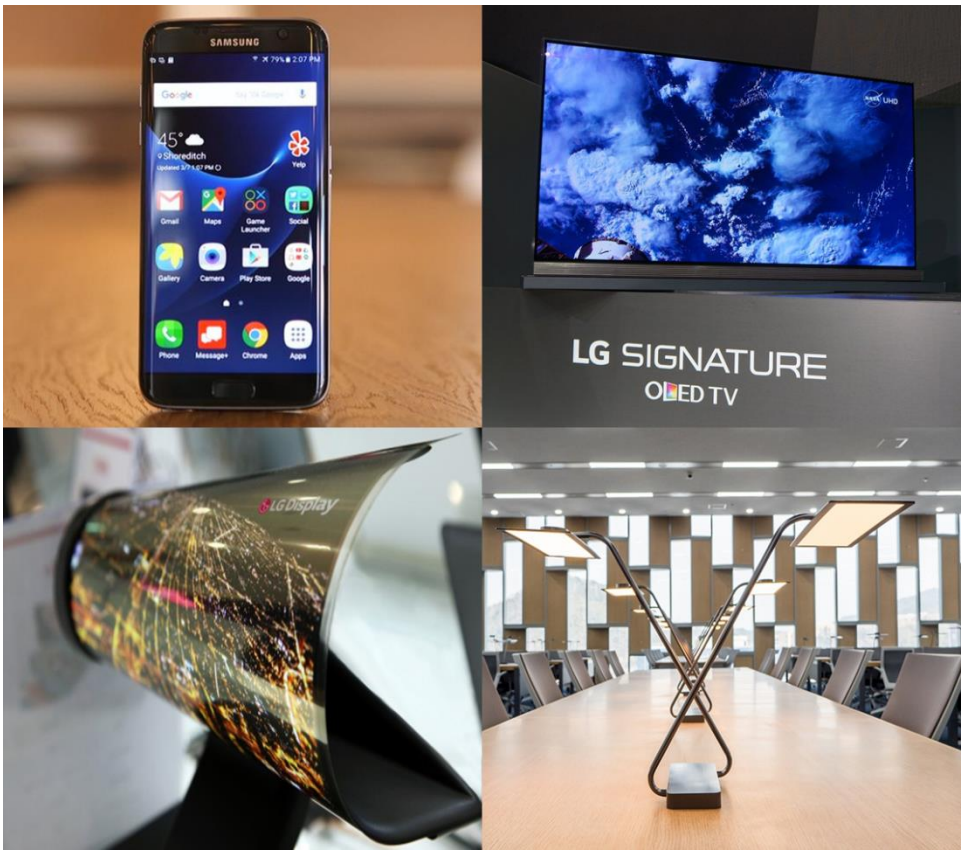

Figure 1.1 Various application products of OLEDs. Samsung mobile display, LG TV display, LG Chemical solid state lighting, LG Display flexible display (clockwise)

The first observation of electroluminescence (EL) in organic materials was reported by Pope, Kallmann, and Magnate in 1963 [1]. However, they used 10 μm to 20 μm thick single crystal anthracene and could observe emitted light from anthracene above about 400 V, which are difficult to use them as a practical product. Vityuk and Mikho established that vapor-deposited thin films of anthracene also exhibit EL [2]. Subsequently, Vincett *et al*. reported clearly visible EL from an organic material at voltages significantly less than 100 V using vacuum-deposited anthracene, but external quantum efficiency (EQE) of the device is about 0.03% ~ 0.06% [3]. Partridge reported first EL generation from organic polymer films [4].

Practically available OLEDs were invented by Tang and VanSlyke in 1987 [5]. The device has a double-layer structure of organic thin films, prepared by vacuum deposition. The aromatic diamine as a hole transporting layer (HTL) and 8-hydroxyquinoline aluminum (Alq_3) as an emitting and electron transporting layer (ETL) were used. Total thickness of the device was approximately 135 nm, which is much thinner than previous reported organic EL devices. The device emitted green color with relatively high EQE (1%) and high brightness (> 1000 cd/m^2) at a driving voltage below 10 V. Tang *et al*. doubled the efficiency of OLEDs in comparison with the undoped device by introducing molecular doping system in 1989 [6]. Moreover, the EL colors can be readily tuned by a suitable choice of dopants as well as by changing the concentration of the dopant. Above works were achieved by using small molecular weight organic materials and the vacuum thermal evaporation technique. In 1990 Burroughes *et al*. reported the first conjugated polymer light-emitting diodes (PLEDs) by spin-coating poly(p-phenylene vinylene) (PPV) on the indium-tin-oxide (ITO) coated glass substrate and the maximum quantum efficiency of the device is about 0.05% [7]. The availability of solution process means that PLEDs have a potential of low-cost fabrication for large-size device compared with vacuum thermal evaporation. Kido *et al*. demonstrated first white OLEDs by using polymer doped with blue, green, and orange fluorescent dyes [8]. Though the efficiency of the device is low, this result suggests that OLEDs can be utilized for illumination devices. After that, there are many efforts such as synthesizing efficient materials and developing novel device structures to improve the efficiency of OLEDs. However, the efficiency of the device was low because they used only fluorescence. When the electrically injected electrons and holes are recombined, the singlet and triplet excited states are generated with the ratio of 1:3, statistically.

Fluorescence utilizes only singlet excitons so the internal quantum efficiency (IQE) of OLEDs with the fluorescent emitter is theoretically limited to 25%.

M. A. Baldo *et al*. dramatically improved the efficiency of OLEDs by the introduction of the phosphorescent dye 2,3,7,8,12,13,17,18-octaethyl-21H,23H-porphine platinum(II) (PtOEP) [9]. Using phosphorescent material means that the IQE of OLEDs can be theoretically 100% because phosphorescence utilizes triplet excitons as well as singlet excitions. Tandem structure using charge generation layers and p-i-n structure using electrical doping also intensely improved the performance of OLEDs [10,11]. Today, the performances of OLEDs are surprisingly enhanced and organic materials with high efficiency and stability are being developed from several companies. The recent status of commercially available OLED emitter materials are summarized in Table 1.1.

Though the performance of OLEDs is improved, there are still many problems to resolve. For example, deep blue phosphorescent materials are not commercially available due to their low efficiency and lifetime. The lifetime of the fluorescent deep blue emitter material is generally longer than that of the deep blue phosphorescent material but its efficiency is lower than that of the phosphorescent materials. Phosphorescent light blue materials have lifetime which covers solid-state lighting sources or displays of mobile phones but cannot covers TVs. Light blue color leads to low color gamut in TV so deep blue phosphorescent materials with high efficiency and long life time are required.

Recent phosphorescent materials show the IQE of 100% but EQE is generally limited to 20% due to an optical loss by glass substrate, ITO, and organic materials. Many researchers have studied to increase out-coupling efficiency by using various methods such as external macro-extractor, micro-lens array, surface scattering layers, low-index grid, high-index substrates, and internal extraction layers [12-16].

Table 1.1 The status of emitting materials for OLEDs

	Color	CIE (x, y)	Efficiency (cd/A)	LT50 (hrs)	Company	Ref.
Fluorescence	Red	(0.67, 0.33)	11	160000	Idemitsu Kosan (CIE, Efficiency: at 10mA/cm^2, LT50: at 1000 cd/m^2)	[17]
	Green	(0.29, 0.64)	37	200000		
	Blue	(0.14, 0.12)	9.9	11000		
Phosphorescence	Deep Red	(0.69, 0.31)	17	250000	Universal Display Corporation (at 1000 cd/m^2)	[18]
	Red	(0.64, 0.36)	30	900000		
	Yellow	(0.44, 0.54)	81	1450000		
	Green	(0.31, 0.63)	85	400000		
	Light Blue	(0.18, 0.42)	50	20000		

1.2 White Organic Light-Emitting Diodes

The history of organic light-emitting diodes (OLEDs) that emit white light started 20 years ago when Kido and coworkers reported that they had succeeded in fabrication OLEDs generating light that contained wavelengths across the entire visible part of the spectrum [8]. These days, international researchers in both industry and academy are developing white OLEDs (WOLEDs) for next generation solid-state light sources and display. LG display retails TV products based on WOLEDs. Also many lighting company started to retail the products of WOLED lighting.

The device efficiency is the single most important parameter describing the performance of any light source and is typically measured in lumen per watt (lm/W). This measure for the efficiency is a photometric unit, meaning that it is scaled to the sensitivity of the human eyes. It should therefore more precisely be referred to as luminous efficacy, although the term efficiency is widely used today. Another frequently used figure-of-merit is the external quantum efficiency (EQE), the average number of photons emitted per unit charge passed through the device.

The improvements of materials, device structures, and light extraction techniques have enabled a tremendous advance in WOLEDs over past 20 years. While the first devices reported by Kido and co-workers had efficiencies below 1 lm/W, today's reported devices surpassed the 100 lm/W. In 2003, WOLEDs reached an efficiency of 15 lm/W and were thus for the first time able to surpass the efficiency of traditional incandescent light bulbs. The important benchmark of 60 lm/W was reached in 2006 [19] and in 2008 researchers at Universal Display announced that WOLEDs with an efficiency in excess of 100 lm/W had been realized under laboratory conditions [13]. In 2011, Reineke et al. reported on WOLEDs which reached efficiency in excess of 120 lm/W [16]. After that many

industrial companies reported WOLEDs having the efficiency exceed 100 lm/W with light extraction technique. Also recently, many OLED lighting products have become commercially available by OSRAM and LG Display etc [20]. Figure 1.2 displays the efficiency evolution of white OLEDs [8,16,19-42].

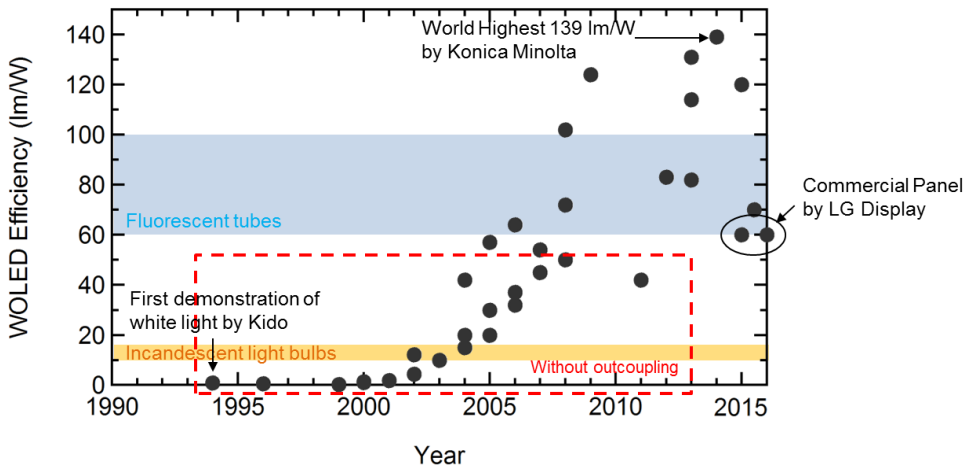

Figure 1.2 Efficiency improvement of WOLEDs over past 20 years. The red box exhibits the results without outcoupling technique.

To obtain the spectral emission characteristics having light covering the entire visible wavelength range, various different approaches has been investigated. The first reported white emitting device had the strategy straightforward way to blend required emitting dye. In 1994 Kido et al. reported that they had successfully realized WOLEDs by doping orange, green, and blue emitting laser dyes in poly(N-vinylcarbazol) (PVK) host [8]. Doping the several dyes in single host matrix have risks that the blend phase-separates over time result in film inhomogeneity, emitting color shift on device driving, and a local increase in current density. Although the blending strategies have the risks on device performance, it generally considered to offer simpler device fabrication than other approaches. Many research groups still investigated on this approach [43,44].

To resolve the major cons of single-EML strategy, the multi-EML structures for white light were discussed. The multi-EML structure allows flexible manipulation of each EML as well as precise control of the exciton distributions or charges in different EMLs and better EL performance can be achieved. However, the more complex structure of device compared to single-EML device is disadvantage. As conventional structure, thin hole and electron blocking layers called as interlayer are inserted in between the emitting layers [45]. To obtain balanced excitation by direct charge recombination, interlayers confine a fraction of the charges inside each of the emissive layers, while allowing a sufficient amount of charge to penetrate into the next EML [37].

The other approach to achieve white emission is arranging a set of complete OLED stacks emitting different colors. From an electrical viewpoint, this means that several independent OLEDs are connected in series called as tandem structure. The motivation for this tandem structure is to increase the current efficiency of the device. Instead of obtaining one photon per injected charge, a tandem OLEDs can generate multiple photons per injected charge. However, this approach comes at the cost of an operating voltage. Therefore the power efficiency of device cannot be higher than conventional device. The tandem structure has many advantages like higher current efficiency, higher color stability, and device lifetime due to its lower driving current density. However, that fabrication steps are doubled compared to conventional devices [46,47].

There are three candidates of emitting materials to obtain white spectral emission. The first choice is fluorescent emitters which have advantages of long device lifetime and material variety. However, fluorescent emitters can only utilize singlet exciton have 25 % portion of generated exciton in emitting layer, meaning the device intrinsically has low efficiency. The second choice is phosphorescent

emitters. Phosphorescent emitters can utilize all of triplet and singlet excitons and exhibit high efficiency. The disadvantage of this choice is the lifetime of blue phosphorescent emitter. To resolve disadvantages of above two choices, hybrid approach, which use blue fluorescent emitter and green, red phosphorescent emitter, is suggested. To realize hybrid type WOLEDs, there are the hurdles of design strategies such as prohibiting mutual exciton transfer and color changes.

In this thesis, the multi-EML structure WOLEDs are discussed. Due to its advantages of device efficiency, easy exciton manipulation, and simple structure compared to tandem approach, it has worth to develop more. Also we used hybrid type emitter choice to resolve the disadvantages of fluorescent and phosphorescent emitters.

1.3 Outline of Thesis

This thesis consists of five chapters including **Introduction** and **Conclusion**. In **Chapter 1**, brief history and research trend of OLEDs. In addition, it also includes the status of WOLEDs and issues. In **Chapter 2**, the fabrication and characterization methods for the OLED devices are summarized. Also, the chemical structures of all used organic materials are demonstrated. In **Chapter 3**, the design strategy of non-interlayer hybrid WOLEDs, using mixed host for blue emitting layer, is demonstrated. Moreover, the effect of mixed host and device stability compared to the device with interlayer are also described. In **Chapter 4**, the stability improvement techniques for blue OLEDs based on TADF material and the degradation mechanisms are described. In **Chapter 5**, we demonstrated the hybrid WOLEDs based on TADF blue emitter. We used mixed host structure demonstrated in **Chapter 4** to improve the device stability and performance. Finally, **Chapter 6** conclude all the thesis.

Chapter 2

Experimental Methods

2.1 Materials

2.1.1 Preparation of Organic Materials

The all organic materials used in the thesis are commercially available and purchased and used without further sublimation. The molybdenum trioxide (MoO_3), lithium fluoride (LiF), and aluminum (Al) were purchased from commercial company (CERAC). Most organic materials were purchased from commercial company (OSM).

2.1.2 Chemical structures of Organic Materials

Below figures are chemical structures of organic materials used in this thesis.

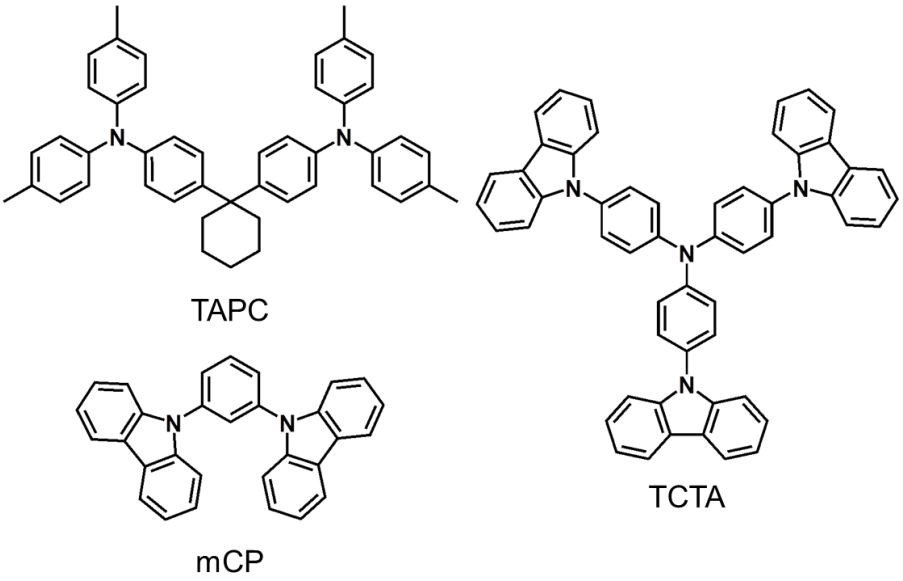

Figure 2.1 Chemical structures of di-[4-(N,N-ditolyl-amino)-phenyl]cyclohexane (TAPC), 4,4',4"-tris(carbazol-9-yl)triphenylamine (TCTA), and 1,3-bis(carbazol-9-yl)benzene (mCP) as hole transporting materials and host materials.

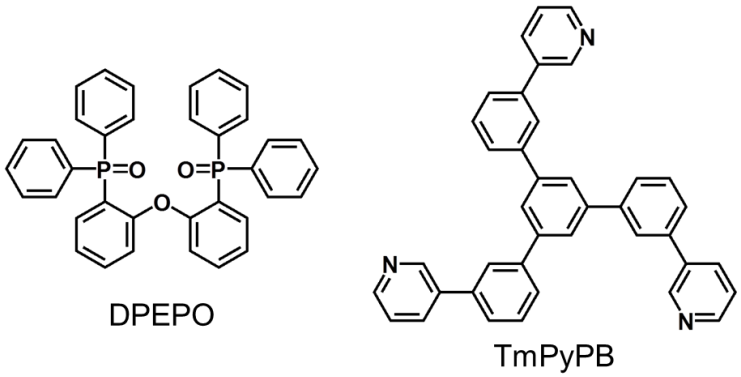

Figure 2.2 Chemical structures of bis[2-(diphenylphosphino)phenyl]ether oxide (DPEPO), and 1,3,5-tri[(3-pyridyl)-phen-3-yl]benzene (TmPyPB) as electron transporting materials and host materials.

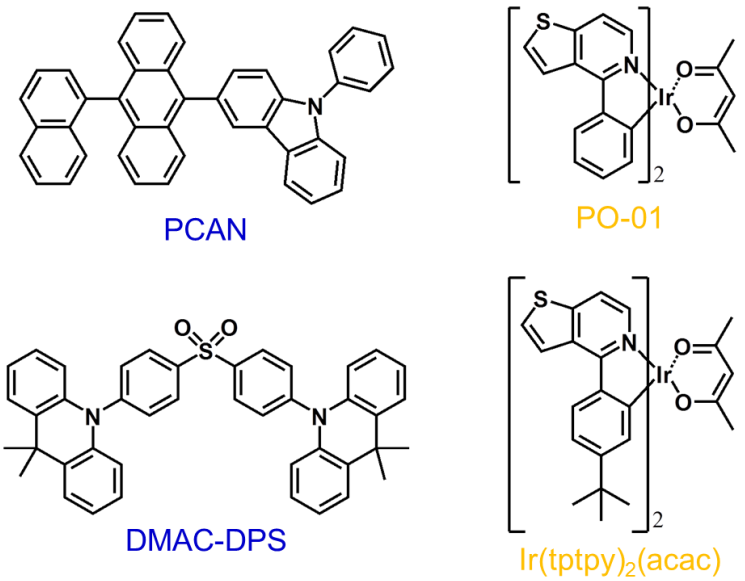

Figure 2.3 Chemical structures of 9-(9-phenylcarbazole-3-yl)-10-(naphthalene-1-yl)anthracene (PCAN), bis[4-(9,9-dinethyl-9,10-dihydroacridine)phenyl]sulfone (DMAC-DPS) as blue emitters, iridium(III)bis(4-phenylthieno[3,2-c]pyridinato-N,C2') acetylacetonate (PO-01), and iridium(III)bis(4-(4-*t*-butylphenyl)thieno[3,2-*c*]pyridinato-*N*,*C*2')acetylacetonate (Ir(tptpy)$_2$(acac)) as yellow emitters.

2.2 Device Fabrication and Characterization Methods

2.2.1 Device Fabrication Methods

All devices used in this thesis have slightly different structures in each chapter to obtain optimized performances. Typical device fabrication methods are as follows: The patterned ITO coated glass substrates were cleaned in ultrasonic bath (Branson 5510) with acetone, isopropyl alcohol, and deionized water. The cleaned substrates were dried in ambient oven at 120 ℃ for more than 1 hour. For the standard structure, ITO coated glass substrates were treated with ultraviolet-ozone cleaner (UVO-42) to remove the surface hydrocarbon contamination and increase the work function of the ITO. The vacuum deposition of thin films was performed by thermal evaporation under a base pressure of 1–5 × 10^{-6} Torr at a rate of 0.2-2 Å/s for organic semiconducting materials, 0.04–0.1 Å/s for LiF (electron injection material), 0.2–0.5 Å/s for MoO_3 (hole injection material) and 3–5 Å/s for Al (metal cathode or anode), respectively. The evaporation speed was monitored with a quartz-oscillator thickness monitor. The doping concentration was adjusted by varying the relative evaporation speeds of the host and dopant materials.

2.2.2 Current-Voltage-Luminance Measurement

Fabricated device was mounted onto the cryostat for the current-voltage-luminance (I-V-L) measurement. The emitting area is 1.4 × 1.4 mm^2 which is defined by the crossing overlap of patterned ITO and Al electrodes. Most of the devices were measured at room temperature.

The current-voltage (I-V) characteristics were measured with a Keithley 236 source measurement unit, while the electroluminescence was measured with a calibrated Si photodiode (Hamamatsu, S5227-1010BQ) with a size of 10 mm × 10 mm placed at an angle normal to the device surface, assuming that the device was a Lambertian source. To detect a turn-on voltage of light-emitting diodes, we use an ARC PD438 photomultiplier tube (PMT) with the Keithley 236 source measurement unit. The electroluminescence (EL) spectra and the Commission Internationale de L'Eclairage (CIE) color coordinates were measured with a Konica-Minolta CS-1000A spectroradiometer. The luminance and efficiency were calculated from the photocurrent signal of photodiode with a Keithley 2000 multimeter, and corrected precisely with the luminance from CS-2000.

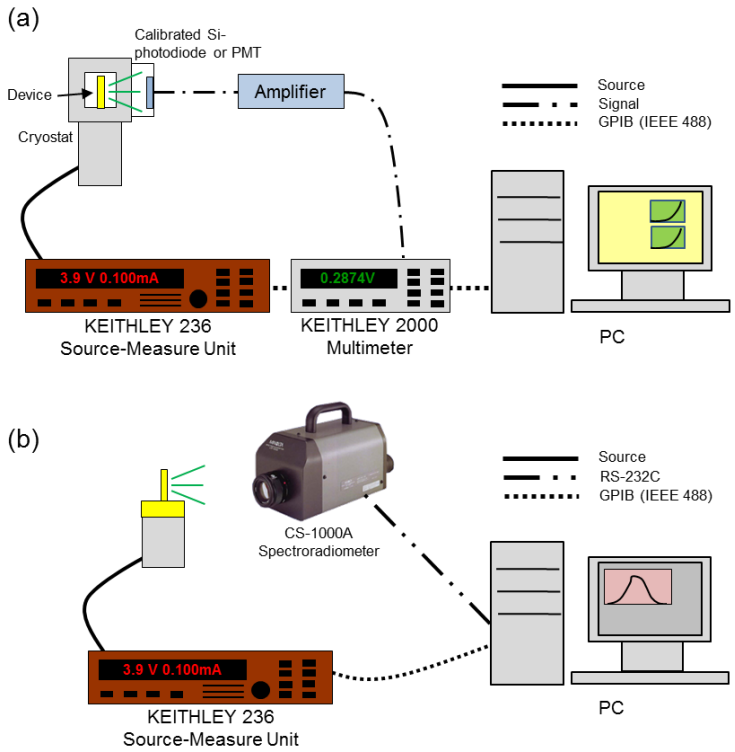

Figure 2.4 Schematic diagrams for the measurement of (a) I-V-L characteristics and (b) EL spectra.

The chromatic characteristics were calculated from EL spectra measured by the CS-1000A spectrometer using the CIE 1931 color expression system. The tristimulus values XYZ can be calculated by following equations,

$$X = K_m \int_0^\infty \bar{x}(\lambda) P(\lambda) d\lambda \tag{2.1}$$

$$Y = K_m \int_0^\infty \bar{y}(\lambda) P(\lambda) d\lambda \tag{2.2}$$

$$Z = K_m \int_0^\infty \bar{z}(\lambda) P(\lambda) d\lambda \tag{2.3}$$

where, P(λ) is a given spectral power distribution of emissive source, $\bar{x}$, $\bar{y}$ and $\bar{z}$ are the CIE standard color matching functions (see Figure 2.2) and Km is the

weighing constant (683 lm W^{-1}). From the tristimulus values, the CIE color coordinates calculated by following equations,

$$x = \frac{X}{X+Y+Z} \tag{2.4}$$

$$y = \frac{Y}{X+Y+Z} \tag{2.5}$$

$$z = \frac{Z}{X+Y+Z} \tag{2.6}$$

Any color can be plotted on the CIE chromaticity diagram.

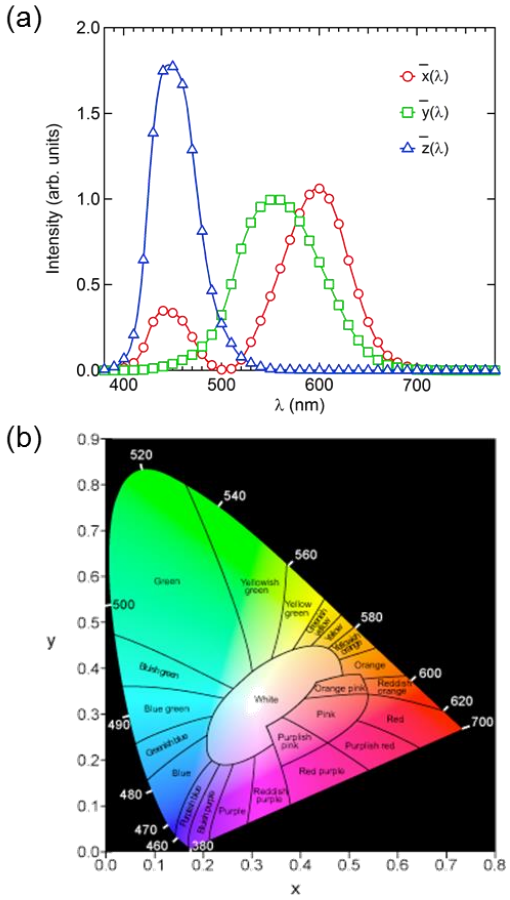

Figure 2.5 (a) The CIE standard observer color-matching functions and (b) the CIE 1931 color space chromaticity diagram. The outer boundary is the spectral locus, with wavelengths shown in nanometers.

2.2.3 Efficiency Calculation Methods

To evaluate the emission properties of light-emitting diodes, the commonly employed efficiencies are the external quantum efficiency (EQE), the luminous efficiency (LE) and the power efficiency (PE).

The external quantum efficiency can be defined by the following equation.

$$\mathrm{EQE} = \frac{number\ of\ emitted\ photons}{number\ of\ injected\ electrons}(\%)$$

Typically, QLEDs or OLEDs emit light into the half plane due to the metal contact. Without any modification for increasing out-coupling efficiency, over 80% of the emission can be lost to internal absorption and wave-guiding in a simple planar light-emitting device.

Since human eye has different spectral sensitivity in visible area, the response of the eye is standardized by the CIE in 1924 (see $\bar{y}$ in Figure 2.2). The luminous efficiency weighs all emitted photons according to the photopic response of human eye. The difference is that EQE weighs all emitted photons equally. LE can be expressed by the following equation.

$$\mathrm{LE} = \frac{luminance}{current\ density}(cd\ A^{-1})$$

The luminance value (cd m^{-2}) can be easily measured by the commercial luminance meter (CS-1000A in this thesis).

The power efficiency is the ratio of the lumen output to the input electrical power as follows,

$$\mathrm{PE} = \frac{luminous\ flux}{electrical\ power}(lm\ W^{-1})$$

The EQEs can be useful to understand the fundamental physics for light emission mechanism, while the PEs can be useful to interpret the power dissipated in a light-emitting device when used in a display application [ref].

2.2.4 Transient Electroluminescence Measurement

The set-up for the transient-electroluminescence (T-EL) measurement is shown in Figure 2.6. The periodic voltage pulse of 10:1 duty is generated from high power pulse generator (Agilent 8114A). 400 μs period was used for all emitters. The electroluminescence signal measured from the PMT is amplified by 1 $k\Omega$ load resistance and captured by 500 Mhz digital oscilloscope (TDS 5054B). In addition, Optional 50 Ω resistance was used to measure the device current and protect circuit when device make short circuit. Time synchronization between electric pulse and measured electroluminescence signal is achieved by the trigger signal from the high power pulse generator. The intensity of the electrical pulse was step-wisely increased to adjust the electric field intensity applied to the devices

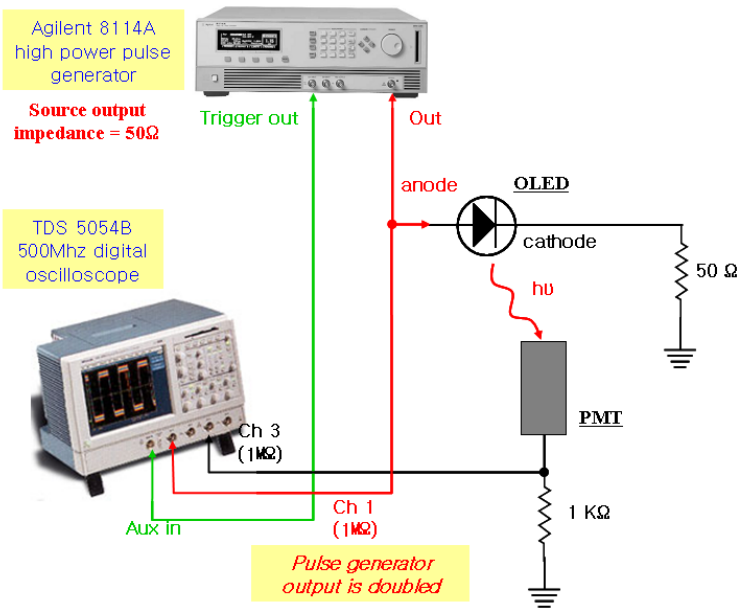

Figure 2.6 The set-up for the transient electroluminescence (T-EL) measurement.

2.2.5 Other Characterization Methods

UV-Visible Spectroscopy: The transmission and absorption spectra were measured with DU-70 UV/Vis Scanning Spectrophotometer (Beckman Coulter, Inc.) or Agilent 8454 UV-Vis. diode array spectrometer. In case of solution, materials were dissolved in toluene or chlorobenzene. For the film measurement, materials were spin-coated or evaporated thermally in the thickness of ~50 nm on quartz substrate. The reflectance spectra were measured by a Varian Cary 5000 spectrophotometer. The average transmittance (T_{avg}) was calculated by the following equation.

$$T_{\mathrm{avg}} = \frac{\int_{\lambda_1}^{\lambda_2} T(\lambda)\mathrm{d}\lambda}{\lambda_2 - \lambda_1} \tag{2.7}$$

Where $T(\lambda)$ is the transmittance as a function of the wavelength, T_{avg} was usually calculated by integrating $T(\lambda)$ from 400 nm (λ_1) to 800 nm (λ_2).

Atomic Force Microscopy (AFM): Topography of each film was measured by XE-100 (Park Systems) AFM System. Most of the films were measured in non-contact mode with NCHR probe tip (320 kHz, 42 N m^{-1}) followed by image processing in XEI v.1.7.1.

Film Thickness Measurement: Ellipsometers (L2W15S830 with 632.8-nm He-Ne laser light, Gaertner Scientific Corp. and M2000D, Woollam) and an AFM (XE-100, Park Systems) were used for measuring the thicknesses of films

Chapter 3

Mixed Host for Efficient Hybrid WOLEDs with non-interlayer structure

The combination of fluorescent and phosphorescent emitters in white OLEDs, which is then called hybrid white, can be advantageous over pure fluorescent or pure phosphorescent white OLEDs, as has already been discussed in **Section 1**. Though pure phosphorescent based white devices are able to show very high efficiency, the deep blue phosphorescent emitter systems still lack high long-term operational stability [48,49]. On the other hand, pure fluorescent white devices are able to show high stability, even with deep blue emission. However, their internal quantum efficiency is limited about 25 % due to intrinsic spin statistics. Therefore, especially the combination of fluorescent blue and long wavelength phosphorescent emitters may result in a good compromise between the high efficiency of phosphorescent emitter systems, and the high long-term stability of fluorescent blue emitter systems.

In order to provide high quality hybrid white systems, blue fluorescent dye and red/green or yellow phosphorescent dye should be utilized simultaneously. However, the small energetic distance between blue and green or yellow emitter causes troubles in utilizing excitons. Further, if the blue emitter is fluorescent, and has a singlet-triplet splitting larger than these 0.5 eV meaning low triplet energy level, then its triplet exciton energy is lower than that of a phosphorescent yellow emitter, which means that it efficiently quenches the phosphorescence emission, if excitons are transferred to its triplet state.

Triplet excitons are transferred via diffusion and Dexter energy transfer. Since Dexter energy transfer requires spatial overlap of the molecular orbitals of donor and acceptor, it can be suppressed by placing the emitters in separate emission layers and introducing an interlayer between them. This interlayer should be able to confine the triplets within the long wavelength phosphorescent emission layer, i.e., it should itself have higher triplet energy than the phosphorescent emitter. Simultaneously, it is advantageous if it also has higher singlet energy than the fluorescent blue emitter, such that it also confines the singlet excitons. By this, Förster energy transfer of singlets from the blue to the long wavelength emission layer is reduced, which makes it is easier to achieve a balanced white emission [50].

However, the use of the interlayer has several disadvantages that limit the device performances. First, the voltage drop across the interlayer cannot be neglected, leading to power efficiency (PE) loss. Moreover, the addition of an interlayer brings additional interfaces which inevitably increase the possibility of exciplex formation which diminish the efficiency of hybrid WOLEDs. Finally it also increases device fabrication steps. Therefore, if mutual quenching in a non-interlayer structure can be controlled well, the efficiency would be further improved [51].

In this chapter, we proposed architecture for achieving high performance multi-EML hybrid WOLEDs that does not have conventional interlayer structure. The main concept is to adopt mixed-hosts for the fluorescent blue emission layer (EML) in order to manipulate exciton distribution. Also we compared the performances of devices with and without interlayer.

3.1 The determination of interlayer composition for efficient hybrid WOLEDs

The hybrid WOLED stacks fabricated in this section have the emission layers composed of blue fluorescent and yellow phosphorescent layers. We used 9-(9-phenylcarbazole-3-yl)-10-(naphthalene-1-yl)anthracene (PCAN) as fluorescence blue emitter due to its high performance deep-blue emission. As the yellow phosphorescence emitter, we used bis(4-(4-t-butylphenyl)thieno[3,2-c]pyridinato-N,C20)acetylacetonate ($Ir(tptpy)_2(acac)$). At the interface between two emission layers, exciton transfer may occur due to the low triplet energy level of blue fluorescent emitter. These energy transfers are dealing with interlayers between two emission layers to suppress unfavorable exciton transfer. Figure 3.1 shows the energy transfer paths each directed to the lower energy state. Thermally activated back transfer may also occur, however, this probability is low due to the large energy level difference.

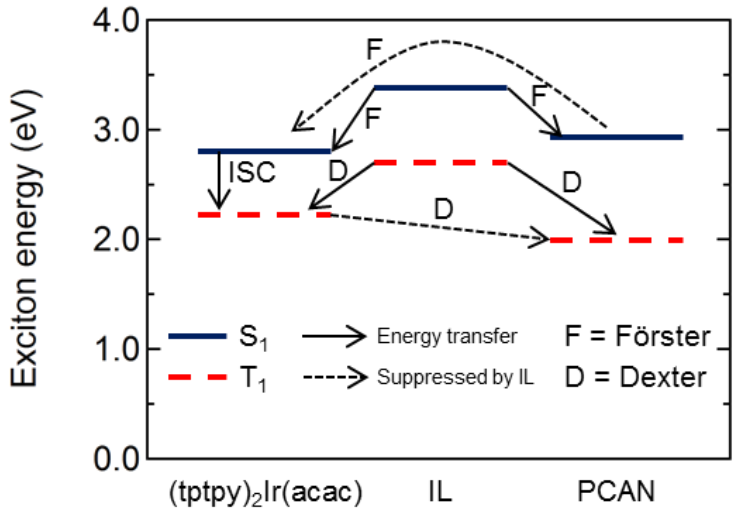

Figure 3.1 Exciton energy diagram and energy transfer mechanisms possible in electroluminescence (EL) process of hybrid WOLEDs with interlayer

The hybrid WOLEDs fabricated in the study were composed of 150 nm indium tin oxide (ITO) as an anode, a 10 nm thick MoO_3 as a hole injection layer, a 50 nm of 1,1-bis[(di-4-tolylamino)phenyl]cyclohexane (TAPC) as a hole transport layer, a 30 nm of 1,3,5-tri(m-pyrid-3-ylphenyl)benzene (TmPyPB) as an electron transport layer, a 0.7 nm thick layer of lithium fluoride (LiF) as an electron injection layer, and a100 nm layer of aluminum (Al) as a cathode. The structure of EML fabricated in this study is displayed in Figure 3.2

The interlayer suppresses unfavorable exciton transfer between yellow phosphorescence emitter and blue fluorescence emitter and manipulates exciton distribution which affect to emission spectra. To find out optimal interlayer structure, we adopted bipolar mixed layer which mixed TCTA hole transporting material and TmPyPB electron transporting material.

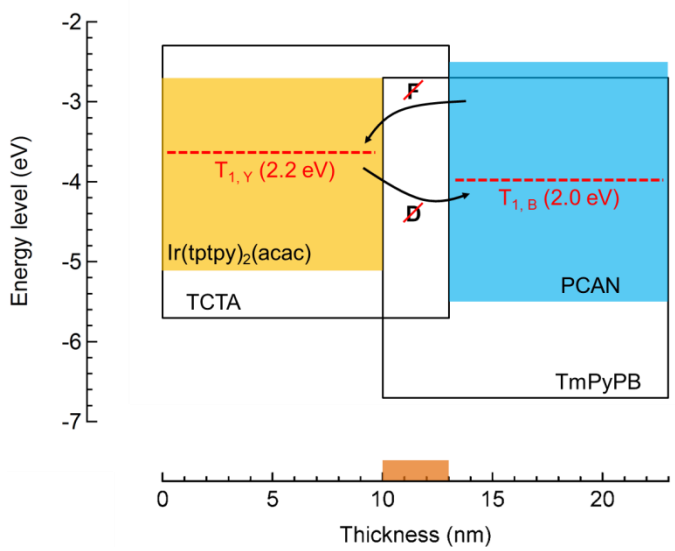

Figure 3.2 The structure of EML proposed on this study

The mixing ratio of the TCTA : TmPyPB blend has an influence on many characteristics of the hybrid white devices. Figure 3.3 shows the EL spectra for the devices with 3 nm interlayers with respect to various mixing ratio. The device without interlayer exhibited strong yellow emission with almost no blue emission. The TCTA only interlayer yields a large amount of blue emission which is understandable as the high hole mobility. On the contrary, TmPyPB interlayer yields a large amount of yellow emission with very small blue emission. When we adopted the interlayer of 2 : 1 TCTA : TmPyPB blend yields high external quantum efficiency (EQE) and proper white emission spectrum with Commission Internationale de L'Eclairage (CIE) coordinates of (0.40, 0.38).

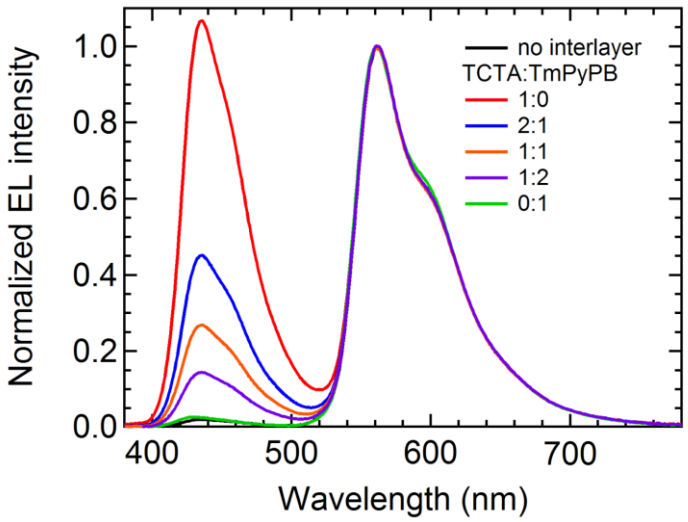

Figure 3.3 Electroluminescence spectra of hybrid OLEDs with various blend interlayers, measured at 5.1 mA/cm^2. The influence of the interlayer blend is visible

It can be seen from Figure 3.4 that the interlayer significantly affects to the device performance. The device without interlayer suffers from strong quenching processes, as the EQE is lower and efficiency roll-off is large. The device characteristics of all devices fabricated in this section are summarized in Table 3.1.

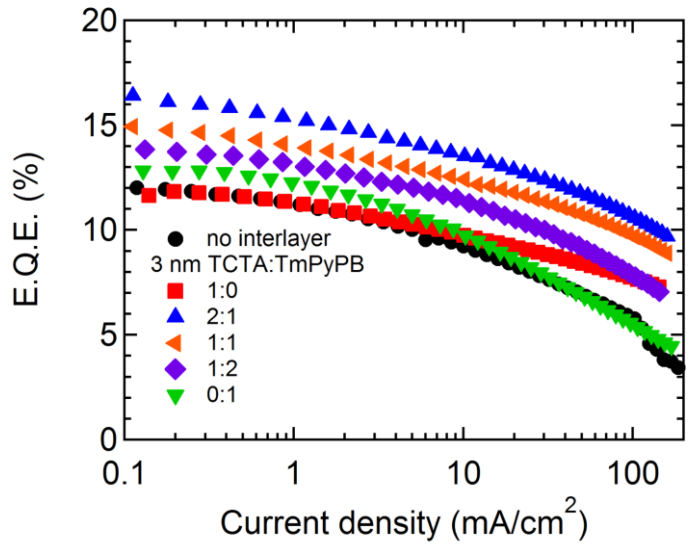

Figure 3.4 External quantum efficiencies of the two-color hybrid white OLEDs. The efficiencies are dependent on the spectrum.

Table 3.1 The various device characteristics of hybrid white OLEDs with respect to interlayer composition.

Device	Max EQE (%)	EQE at 1000 cd/m^2	Max PE (lm/W)	PE At 1000 cd/m^2	V_d (V) At 1000 cd/m^2	CIE1931 (x, y)
No interlayer	12.0	10.4	31.1	20.6	5.1	(0.47, 0.49)
TCTA:TmPyPB 1:0	11.8	10.3	17.5	11.6	5.6	(0.33, 0.29)
TCTA:TmPyPB 2:1	16.3	14.6	34.0	24.8	5.0	(0.40, 0.38)
TCTA:TmPyPB 1:1	14.9	13.4	36.4	26.2	4.7	(0.43, 0.42)
TCTA:TmPyPB 1:2	13.8	12.3	33.2	23.5	4.9	(0.45, 0.45)
TCTA:TmPyPB 0:1	12.8	11.2	32.5	22.3	5.1	(0.48, 0.49)

To analyze the charge transporting characteristics of yellow and blue EML, we fabricated the hole-only-devices (HODs) and electron-only-devices (EODs) with the doping concentration of emitting dyes. Figure 3.5 shows the current density-voltage characteristics of single carrier devices. The doping of yellow dopant decreases hole current density due to the hole trap. On the other hand, electron current increases. This self-charge-trapping effect can contribute to the yellow emission. The blue fluorophore supports the transport of both electrons and holes, which is beneficial to broaden the exciton recombination zone.

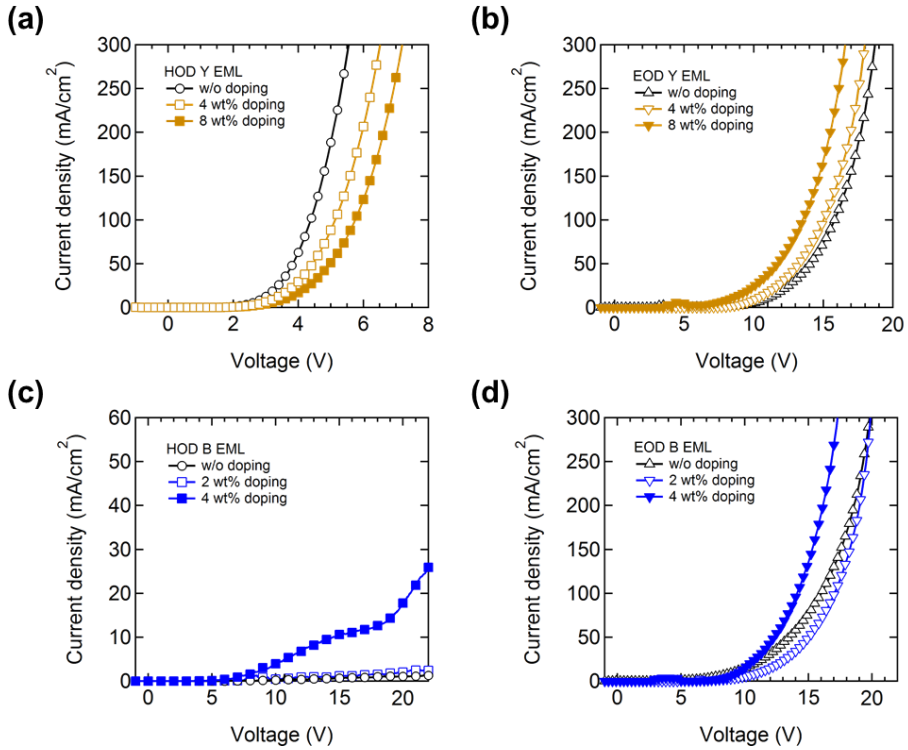

Figure 3.5 The current density-voltage characteristics of (a) hole-only devices of yellow emitters, (b) electron-only devices of yellow emitters, (c) hole-only devices of blue emitters, and (d) electron-only devices of blue emitters. The hole only device structure: ITO/MoO_3 (10 nm)/TCTA (20 nm)/EML (30 nm)/TCTA (20 nm)/MoO_3 (10 nm)/Al. The electron only device structure: Al/LiF (1 nm)/TmPyPB (20 nm)/EML (30 nm)/TmPyPB (20 nm)/LiF (1 nm)/Al

3.2 Non-interlayer hybrid WOLEDs using mixed host for blue EML

As we discussed in **Section 3.1**, we can achieve efficient hybrid white OLEDs using interlayer which modulating exciton distribution and prohibit unwanted exciton energy transfer. However, the insertion of interlayer has several disadvantages that limit the device quantum efficiency and power efficiency. Thus, if mutual quenching in a non-interlayer structure can be controlled well, the efficiency would be further improved.

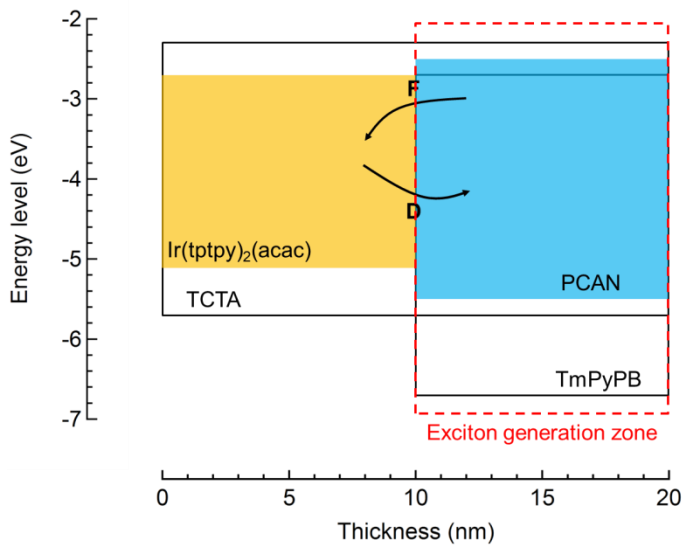

Figure 3.6 Energy level scheme for EML used in the hybrid white OLED, The red box with dotted line exhibits exciton generation zone

Figure 3.6 shows the schematic diagram of EML for non-interlayer hybrid white OLEDs in this section. It is important to precisely control the doping concentration of emitters. In this study, as the blue EML 4 % PCAN doped TCTA was used and as yellow EML 8 % $Ir(tptpy)_2(acac)$ doped TmPyPB was used. In the

non-interlayer hybrid WOLEDs, the critical problem is the mutual exciton quenching between the phosphorescent yellow emitters and the fluorescent blue emitter when directly contact each other. The one possible energy transfer path is Dexter energy transfer from the triplet state of $Ir(tptpy)_2(acac)$ (T_1: 2.2 eV) to the lower lying non-radiative triplet state of PCAN (T_1: 2.0 eV), resulting in energy loss and thus a reduction in device efficiency. On the other hand, the singlet excitons in blue EML can undergo a direct radiative decay to blue emission or be transferred via Förster energy transfer to yellow EML to enhance the yellow emission. Although, this Förster energy transfer is not a loss mechanism, it would lead to the insufficient blue emission. The direct contact of yellow phosphors perturbing the utilization of the singlet excitons for blue emission has a negative effect on the white light. In order to resolve this issue, we employed 2 : 1 TCTA : TmPyPB mixed bipolar host for PCAN blue fluorescent emitter, which is the key feature of this structure. The other structure of the device was same as the devices in **Section 3.1**. To prove the effect of mixed host for removing interlayer, the optimized device was compared with the interlayer device in **Section 3.1**.

Figure 3.7 shows the device characteristics of two hybrid WOLEDs, conventional interlayer structure and non-interlayer structure. It is obvious that the additional thick interlayer increases the driving voltage, which limits the PE. The maximum EQE and PE of non-interlayer device were 17.1 % and 36.4 lm/W, respectively. It is higher than those of the device with interlayer which were 16.4 % and 36.0 lm/W, respectively. At the practical luminance of 1000 cd/m^2, they still remain as high as 16.3 % and 25.3 lm/W in non-interlayer device, exhibiting still higher compared to those of interlayer device which were 13.5 % and 20.1 lm/W. However, the critical current density J_c, where EQE declines by half from its maximum [52], of non-interlayer device was 74 mA/cm^2 which is lower than that of

the device with interlayer, 187 mA/cm^2. Figure 3.8 shows the current density dependent EL spectra of devices. It clearly shows the color shifts of all devices were small, changes in CIE coordinates of < (0.01, 0.01), indicating balanced exciton generation. Table 3.2 summarized the EL performances of the hybrid WOLEDs in previous studies. We could find that the EL performance of our non-interlayer device is impressive without any blue fluorophore having high triplet energy level.

Table 3.2 Comparison of the device performances of the previously reported hybrid WOLEDs a: single-EML, b: multi-EML

	T_1 of Blue emitter	EQE max	EQE 1000 cd/m^2	PE max	PE 1000 cd/m^2	CIE
[53]b	2.6 eV	16.4 %	15.1 %	42.1 lm/W	26.3 lm/W	(0.46, 0.49)
[54]a	2.4 eV	26.6 %	21.2 %	67.2 lm/W	33.5 lm/W	(0.47, 0.44)
[51]b	2.3 eV	23.0 %	17.5 %	51.7 lm/W	34.3 lm/W	(0.44,0.44)
	< 2.0 eV	16.5 %	15.7 %	40.3 lm/W	27.0 lm/W	(0.43, 0.43)
[55]b	< 2.0 eV	16.3 %	-	41.0 lm/W	-	(0.38, 0.46)
[56]a	2.4 eV	15.6 %	-	39.5 lm/W	19.7 lm/W	(0.41, 0.46)
[57]a	2.6 eV	16.5 %	-	46.8 lm/W	-	(0.42, 0.46)
[58]b	<2.0 eV	13.8 %	13.7 %	32.0 lm/W	27.1 lm/W	(0.43, 0.43)
[50]b	2.3 eV	16.1 %	12.9 %	37.5 lm/W	28.0 lm/W	(0.44, 0.47)
This work	**2.0 eV**	**17.1 %**	**16.3 %**	**36.4**	**25.3**	**(0.40, 0.38)**

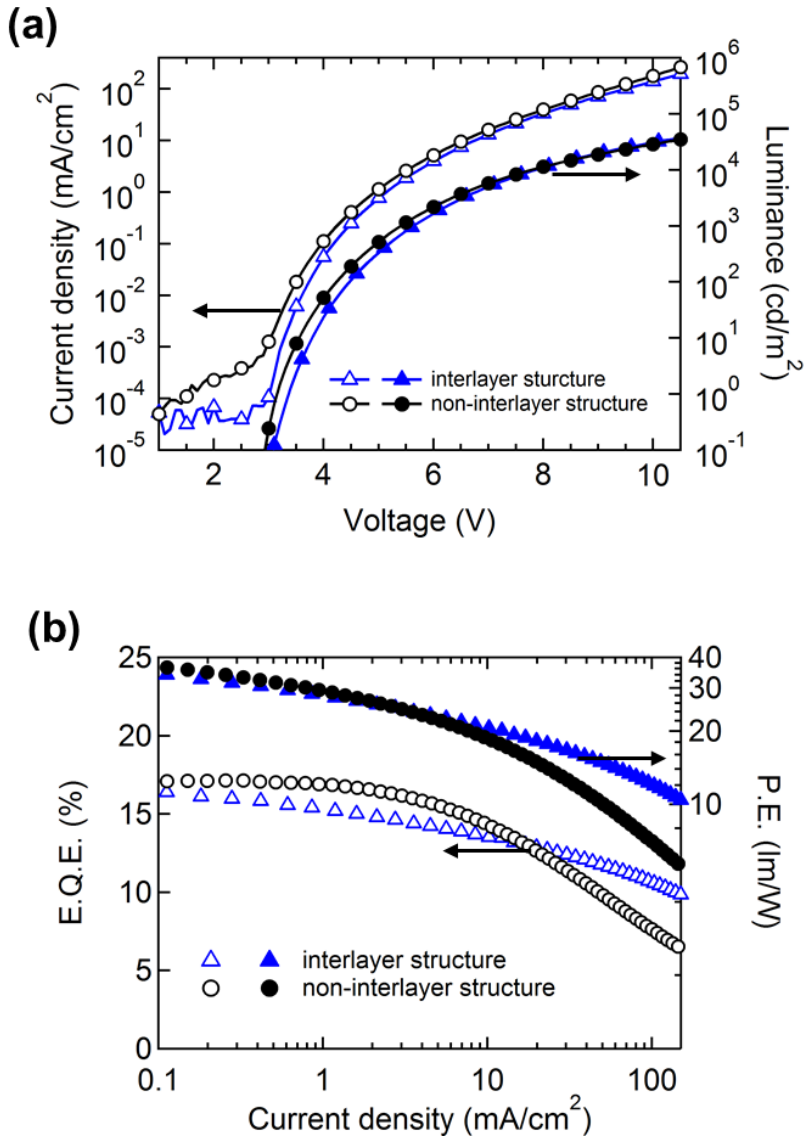

Figure 3.7 (a) Current density-voltage-luminance characteristics and (b) external quantum efficiency and power efficiency versus current density characteristics

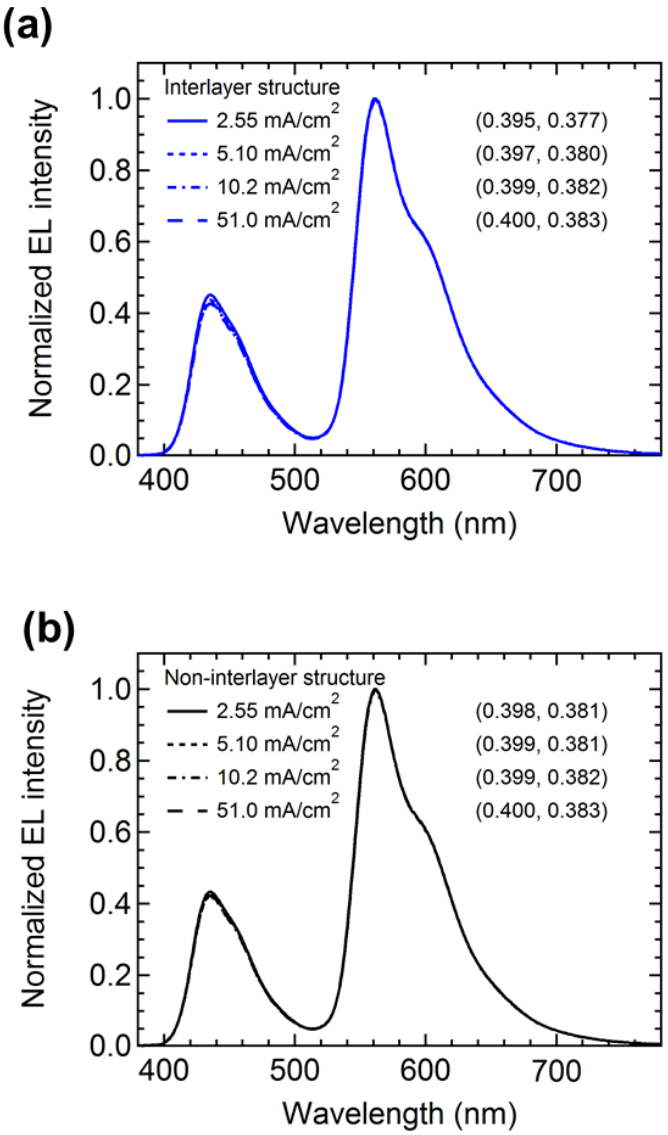

Figure 3.8 The normalized EL spectra at different current density levels of (a) interlayer structure, and (b) non-interlayer structure hybrid WOLEDs

To prove the positive effect of the bipolar mixed host in the blue EML to remove the interlayer, we fabricated two other devices for comparison (See Figure 3.9). Except the variation of the blue EML structure, all other parameters of both devices were kept the same as the discussed non-interlayer device. The devices with blue EML hosts as TCTA and TmPyPB would have narrow exciton generation zone due to its abrupt interface between the blue EML and adjacent layer. As shown in Figure 3.9, the strong yellow emission with negligible blue emission in the device with TmPyPB host because the recombination zone is located at the interface of blue EML and yellow EML and the singlet excitons in the blue EML are largely quenched by yellow phosphor. Alternatively, the device with TCTA host exhibited strong blue emission which suggests that the main recombination zone is located near the blue EML and ETL interface, which is far away from the yellow phosphor containing layer. Furthermore, it can be seen that both devices show significant efficiency roll-off which can be attributed to the quenching effect of space charge accumulation and high density of triplet excitons in narrow exciton generation zone. On the other hand, the non-interlayer device with mixed host has the main exciton generation zone located across the whole blue EML where the majority of injected holes and electrons meet with each other due to the transport properties of mixed host.

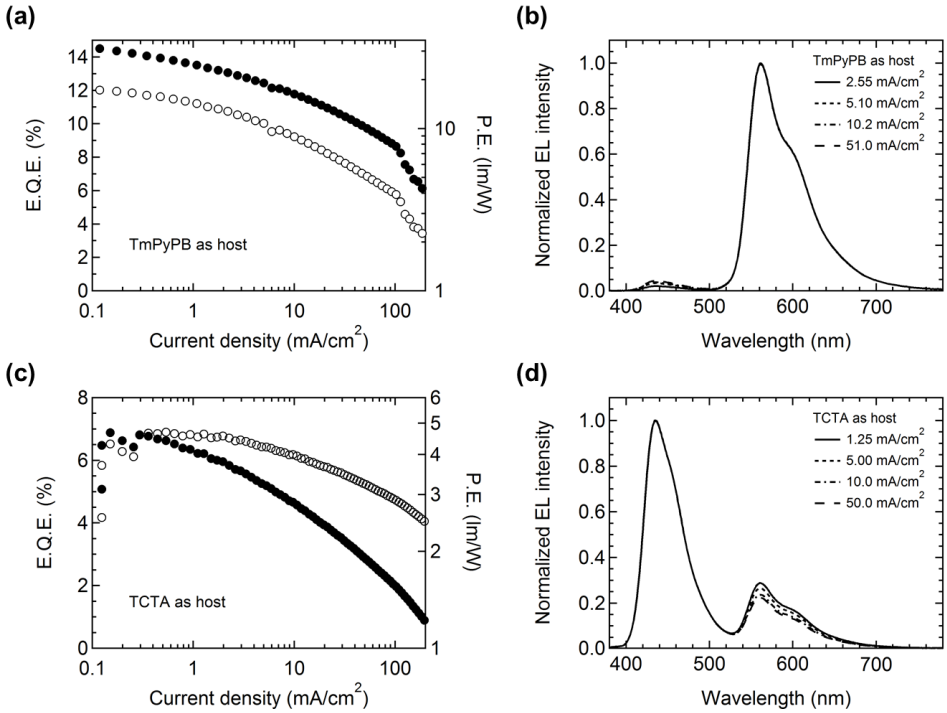

Figure 3.9 (a) External quantum efficiency and power efficiency versus current density characteristics, (b) normalized EL spectra of white device with TmPyPB as blue emitting layer host. (c) and (d) show those of white device with TCTA as host.

It can be assumed that the triplet excitons generated in blue EML with mixed host can diffuse into adjacent yellow phosphor by Dexter energy transfer. Taking into account the fact that the triplet energy level of TmPyPB (2.78 eV) is lower than that of TCTA (2.83 eV), the triplet excitons might diffuse through TmPyPB molecules. To prove this explanation, the device A and B are discussed as shown in Figure 3.10. We can see the green emission from $(ppy)_2Ir(acac)$ phosphorescent emitter in device B. Whereas, the device A shows only negligible green emission. This experimental fact provides the evidence for explanation that triplet excitons generated in blue EML can diffuse through TmPyPB molecules. Meanwhile, to elucidate the efficiency enhancement of non-interlayer device, we assumed that partial triplet excitons on the non-radiative triplet state of PCAN can contribute to yellow emission via the endothermic energy transfer. If the triplet excitons on the triplet state of PCAN can emit via the endothermic energy transfer, the delayed component of yellow emission may exist in transient EL decay curve. To prove the hypothesis, we fabricated the device without PCAN blue emitter which has same architecture with non-interlayer device except nonexistence of PCAN blue emitter. However, as shown in Figure 3.11, there was no delayed component on yellow emission in two devices, indicating that the endothermic energy transfer does not contribute to efficiency enhancement.

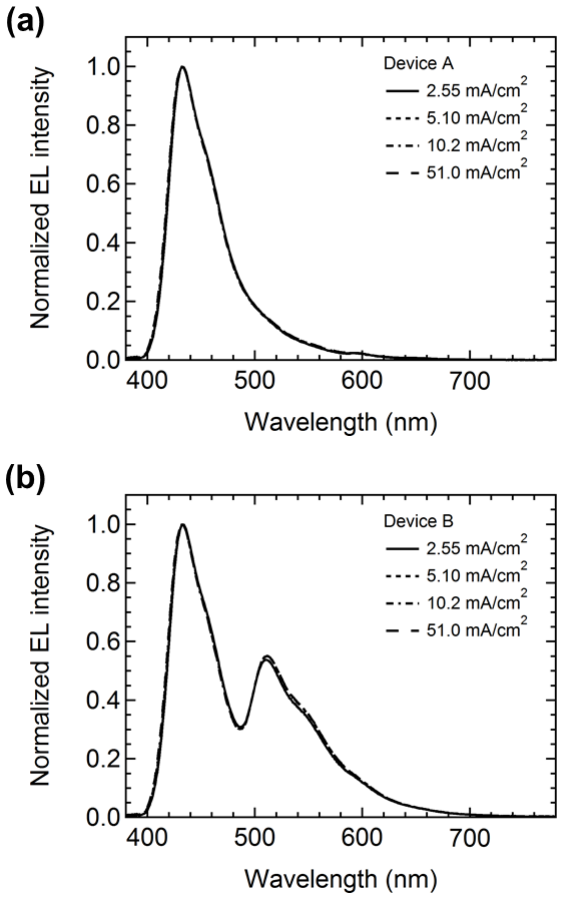

Figure 3.10 The normalized EL spectra for (a) device A with structure of ITO/TAPC/TCTA (5 nm)/$(ppy)_2Ir(acac)$ (0.1 nm)/TCTA (5 nm)/TCTA:TmPyPB:PCAN (2:1, 4 %, 8 nm)/TmPyPB (30 nm)/LiF/Al and (b) device B with structure of ITO/TAPC/TCTA (10 nm)/TCTA:TmPyPB:PCAN (2:1, 4 %, 8 nm)/TmPyPB (5 nm)/$(ppy)_2Ir(acac)$ (0.1 nm)/TmPyPB (25 nm)/LiF/Al.

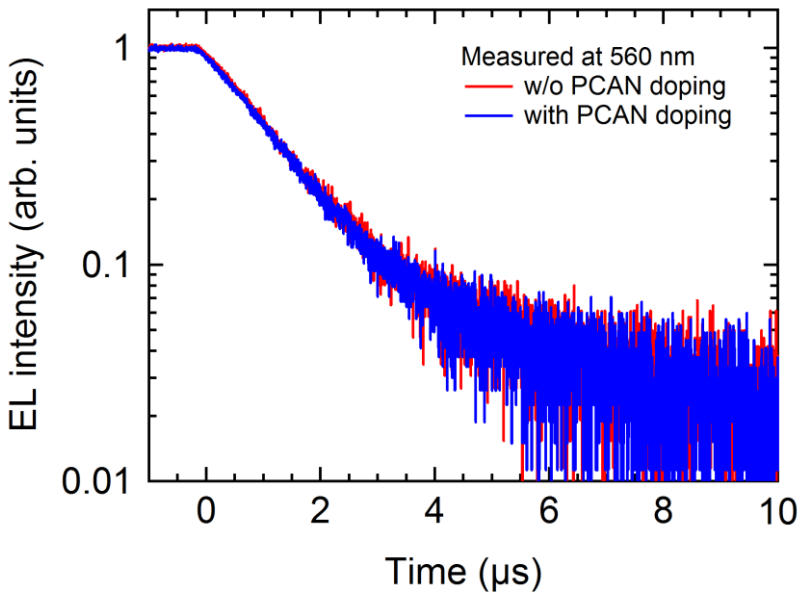

Figure 3.11 Transient EL decay profile measured at 560 nm of the devices with and without PCAN doping.

3.3 Influence of blue EML host structure to white device stability

To commercialize white OLEDs, the stability of the device is important. The hybrid white OLEDs are introduced to achieve long lifetime using the fluorescent blue emitter. In this section, we demonstrated the device lifetime with dependent to the host structure of blue EML and interlayer.

We demonstrated the effect on the device lifetime of removing interlayer for hybrid WOLEDs. The Figure 3.11 displayed the device lifetime characteristics and the measurement carried out at initial luminance 3000 cd/m^2. As a result, the device lifetime LT50 of non-interlayer hybrid WOLED was 1.1 h which was lower than that

of the device with interlayer of 4.0 h. Also it corresponds to the trend of efficiency roll-off properties. In the non-interlayer hybrid WOLED, the inevitable mutual energy transfer between blue fluorophore and yellow phosphor could affect to the device stability. To clarify this result, the non-interlayer device with 2 % PCAN doping concentration was compared. Due to the low concentration of PCAN, the possibility of energy transfer between blue and yellow EML was reduced. The device with lower PCAN concentration exhibited enhanced lifetime of 1.9 h and higher critical current density J_c of 139 mA/cm^2. However, it still has lower lifetime than that of interlayer device, indicating that further study is necessary for enhancing the stability of non-interlayer hybrid WOLEDs.

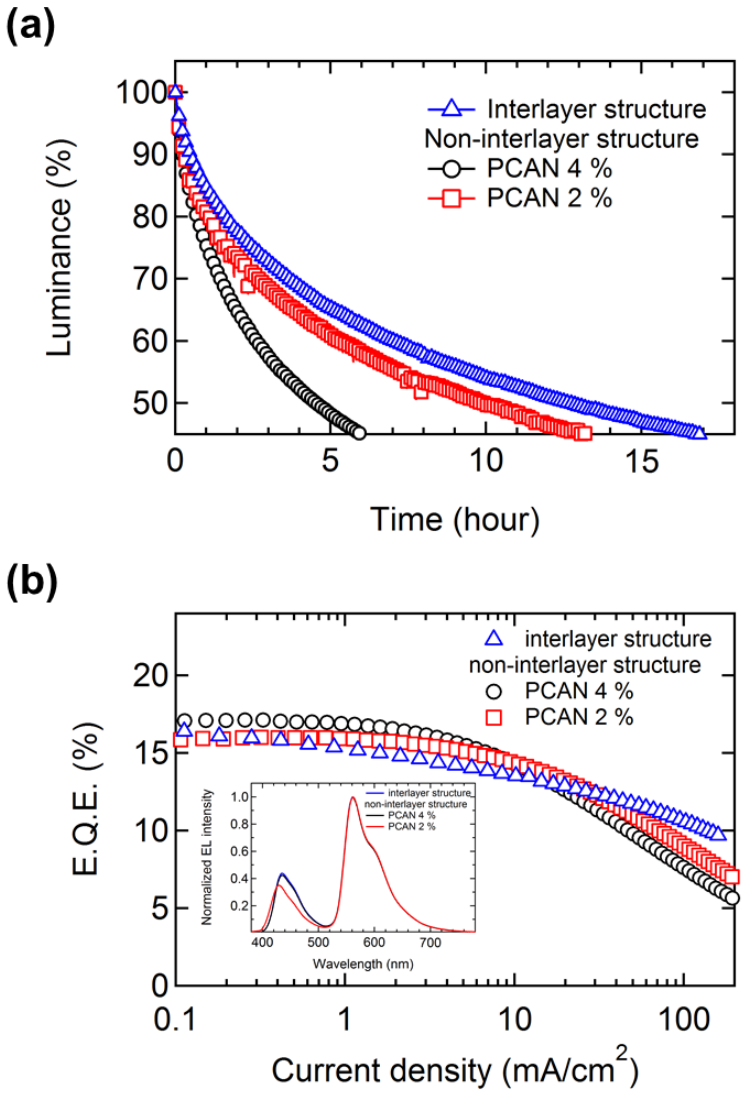

Figure 3.12 (a) The lifetime of fabricated devices, and (b) the external quantum efficiency versus current density characteristics. The inset shows the normalized EL spectra

3.4 Summary

In summary, we investigated improved performance of hybrid WOLED by adopting mixed host with non-interlayer structure. First, we demonstrated the optimization processes of interlayer to achieve high performance hybrid WOLEDs. The interlayer composition of TCTA : TmPyPB with 2 : 1 mixing ratio results in the maximum EQE as 16.4 % and CIE coordinates of (0.40, 0.38). Second, we proposed the design strategy for non-interlayer hybrid WOLEDs using mixed host on blue EML. The mixed host affects to exciton generation zone position to suppress unwanted mutual energy transfer between fluorescent blue and phosphorescent yellow EML. Resulting device exhibited the maximum EQE as 17.1 % with superior color stability depend on the driving current density, indicating efficient non-interlayer hybrid WOLEDs can be utilized by using mixed host on blue EML. We could find that the EL performance of our non-interlayer device is impressive without any blue fluorophore having high triplet energy level. However, the lifetime of non-interlayer device which has LT50 as 1.1 h was worse compared to that of the device with interlayer (LT50 ~ 4.0 h). Inevitable mutual quenching between direct contact of blue and yellow EML pointed out as the cause of this result. The further study is necessary for enhancing the stability of non-interlayer hybrid WOLEDs.

Chapter 4

Improved Device Stability of TADF Blue OLEDs by Adopting Mixed Host System

Organic light-emitting diodes (OLEDs) based thermally activated delayed fluorescence (TADF) molecules have attracted great attention due to their high electron to photon conversion efficiencies [59-61]. Because TADF molecules have very low energy gaps < 0.2 eV between their singlet (S_1) and triplet energy states (T_1), thermally activated reverse intersystem crossing from T_1 to S_1 occurs effectively [62-64]. Therefore, TADF based OLEDs exhibit nearly 100 % of internal quantum efficiencies because both singlet and triplet excitons are almost completely converted into photons under electrical excitation [65,66]. The phosphorescent OLEDs are promising structure producing 100 % of internal quantum efficiencies.

However, phosphorescent emitters contain rare-earth metal such as Iridium (Ir) or Platinum (Pt). In TADF emitters which do not require these rare-earth metals, the lack of rare-earth metals is a great advantage that reduces the material costs for OLEDs. External quantum efficiencies (EQE) of TADF OLEDs have already reached 30 %, which is close to the theoretical limit of EQE [66]. Recently, green TADF OLEDs with 2800 hours half lifetime with initial luminance 1000 cd/m^2 was reported. However, this value is not sufficient for commercial applications and especially blue TADF OLEDs still have very low half lifetime [67,68]. Though many groups have made multidisciplinary efforts to developing stable molecules, the device structural development for enhancing device lifetime is still needed.

In this section, we evaluated the degradation mechanisms of TADF blue OLEDs with mixed host system. To achieve enough device performance with high stability, we used widely reported bis(2-(diphenylphosphino)phenyl)etheroxide (DPEPO) and *m*-bis(N-carbazolyl)benzene (mCP) as host materials. Due to its high triplet energy level 3.3 eV and 3.0 eV, respectively, we could achieve enhanced stability and low efficiency roll-off in TADF blue OLEDs.

4.1 The effect of mixed host structure on blue OLEDs based on TADF emitter

To study the effect of mixed host structure in the blue OLEDs based on TADF emitter, we used bis[4-(9,9-dimethyl-9,10-dihydroacridine)phenyl]sulfone (DMAC-DPS) as TADF blue emitter. Adachi group reported this material as highly efficient TADF blue emitter material, which exhibited 20 % EQE with DPEPO as host similar with that of phosphorescent blue OLEDs [69]. Although, it exhibited superior EL performance, they reported that the half lifetime of blue OLED shows about ~ 1 h with initial luminance of 500 cd/m^2 [69]. The reliability problem is mainly comes from the host material instability [70]. The TADF blue emitters generally have wide emission spectra with short wavelength emission, which produce the necessity of the high triplet energy host materials. However, we still surfer the unavailability of stable high triplet energy charge transport materials. Thus, we tried to resolve this problem of host material selection on blue TADF based OLEDs by using mixed host system.

The energy level diagrams of the blue OLEDs studied in this section are shown in Figure 4.1. The fabricated devices were composed of a 150 nm thick of ITO as an anode, a 10 nm thick layer of MoO_3 as a hole injection layer, a 30 nm thick of TCTA as a hole transport layer, a 20 nm of emission layer of 10 % DMAC-DPS doped mCP and DPEPO mixed host sandwiched between the 10 nm of mCP and DPEPO as exciton blocking layer, a 30 nm of TmPyPB as an electron transport layer, a 0.7 nm LiF as an electron injection layer, and a 100 nm thick of Al as a cathode. The EML structures were varied by the mixing ratio of mCP and DPEPO. To investigate the effect of hole and electron current stress on the OLED degradation, we also fabricated HODs and EODs (Figure 4.1 c,d). The device structure of the HODs was

glass substrate / ITO / MoO_3 (10 nm) / TCTA (30 nm) / EML (20 nm) / TCTA (30 nm) / MoO_3 (10 nm) / Al. The MoO_3 layer with a deep work function of 5.6 eV was inserted between the TCTA and Al or ITO to prevent electron injection from electrodes. The EOD structure was glass substrate / ITO / TmPyPB (30 nm) / EML (20 nm) / TmPyPB (30 nm) / LiF (0.7 nm) / Al. The TmPyPB layer with deep HOMO level of 6.7 eV was inserted between ITO and EML to prevent hole injection.

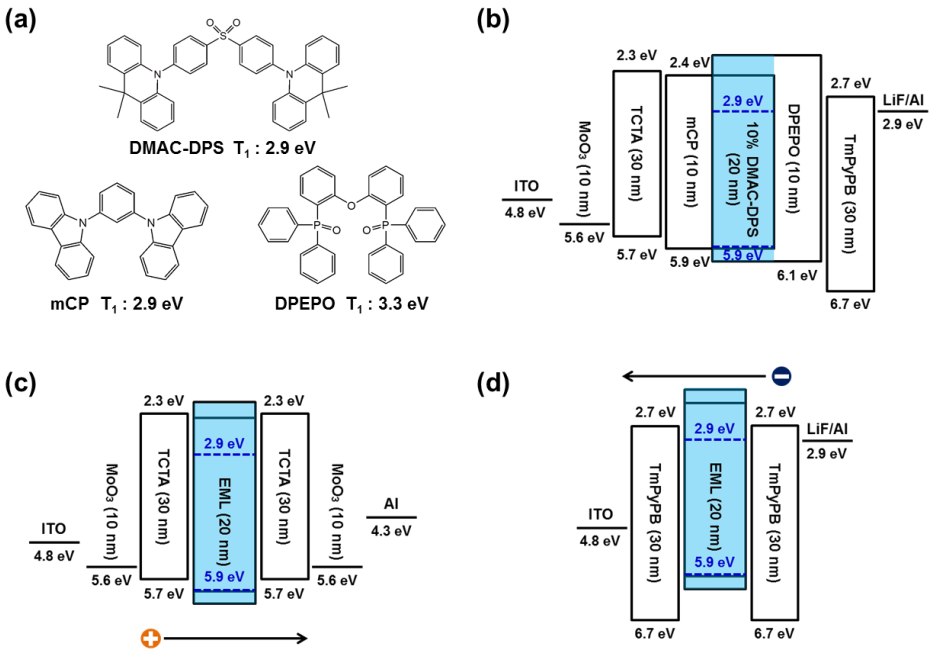

Figure 4.1 (a) Chemical structures of the DMAC-DPS, mCP, and DPEPO and energy level diagram of (b) TADF based OLEDs, (c) HODs, and (d) EODs.

The J-V and L-V characteristics of the fabricated OLEDs are shown in Figure 4.2. Figure 4.3 displays the efficiencies and lifetime of devices. The device with mCP as host shows high current density but it shows a low EL performance because the intermolecular π-π stacking between carbazole units cannot be avoided in mCP film, which formed triplet trap species and quenched the emission of DMAC-DPS [71]. Conversely, the device with DPEPO as host shows the lowest current density due to its low electron mobility. The enhanced EL performance is due to the high T_1 level of DPEPO and weak intermolecular interaction with DMAC-DPS [71]. It is clear that the devices with mixed hosts exhibited the current density higher than the device with DPEPO host, and the enhanced EL performance compared to that of device with mCP host. The maximum EQEs of devices were 11.5 %, 16.2 %, 20.0 %, 21.5 %, and 21.4 % for mCP, mixed host 2 : 1, 1 : 1, 1 : 2, and DPEPO as host, respectively. As increasing DPEPO concentration, the device efficiency also increases because DPEPO reduced the intermolecular interaction between mCP and DMAC-DPS. It is obvious mixed host reduced high current density luminance roll-off of device results in the low efficiency roll-off. The critical current density J_c, where EQE declines by half from its maximum of devices were 22.0, 21.0, 25.2, 17.9, and 9.9 mA/cm^2 for mCP, mixed host 2 : 1, 1 : 1, 1 : 2, and DPEPO as host, respectively. It is because the mixed host broadens the exciton generation zone. We also find out that the device stability is enhanced by mixed host. The device with mCP and DPEPO as single host structure have LT50 25.0 min and 35.5 min respectively. The best stability device is mCP : DPEPO 1:1 device with 61.4 min of LT50. Table 4.1 and Figure 4.4 summarized the properties of fabricated devices.

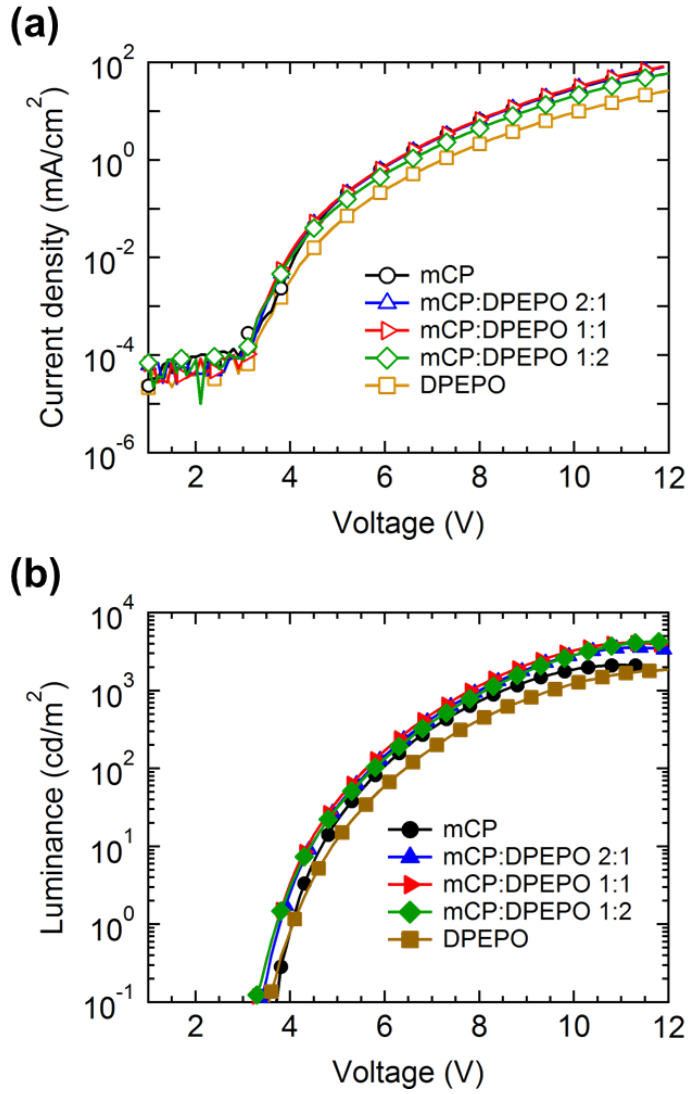

Figure 4.2 (a) Current density versus voltage (J-V) characteristics and (b) luminance versus voltage (L-V) of TADF based blue OLEDs.

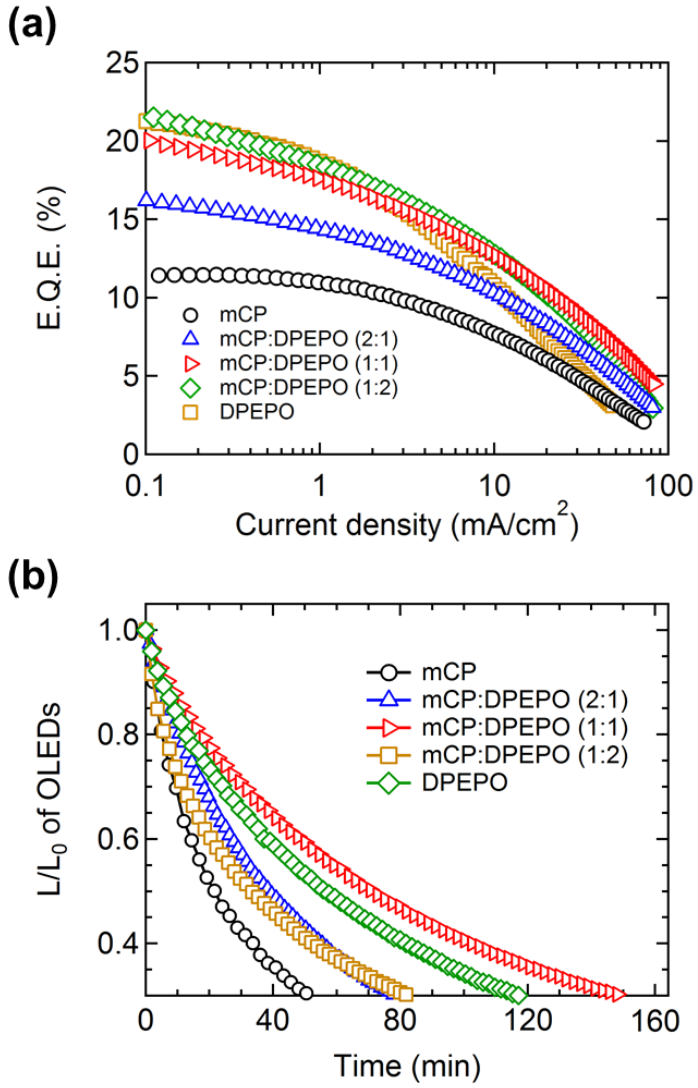

Figure 4.3 (a) External quantum efficiency with respect to current density, (b) the luminance degradation of TADF based blue OLEDs.

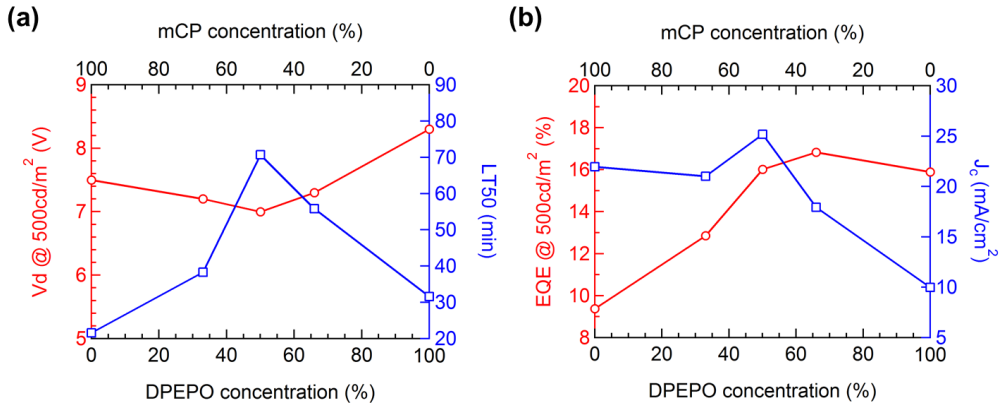

Figure 4.4 Summarized device parameters of (a) driving voltage at 500 cd/m^2 and LT50, and (b) EQE at 500 cd/m^2 and critical current density J_c

Table 4.1 Summary of the parameters of TADF blue OLEDs with mixed host.

Device	Max E.Q.E.	E.Q.E. @ 500 cd/m^2	V_d @ 500 cd/m^2	J_c	LT50
mCP	11.5%	9.4%	7.5 V	22.0 mA/cm^2	25.0 min
mCP:DPEPO 2:1	16.2 %	12.9%	7.2 V	21.0 mA/cm^2	36.5 min
mCP:DPEPO 1:1	20.0 %	16.0%	7.0 V	25.2 mA/cm^2	61.4 min
mCP:DPEPO 1:2	21.5 %	16.8%	7.3 V	17.9 mA/cm^2	50.2 min
DPEPO	21.4 %	15.9%	8.3 V	9.9 mA/cm^2	35.5 min

4.2 Degradation mechanisms of TADF based blue OLEDs

The device stability of TADF based blue OLEDs are dependent on the EML structure. It means that the stability of EML is important features on TADF based blue OLEDs lifetime. We could assume that there are two major degradation pathway of EML. The one pathway is by excited-state stress and the other is degradation by charge carriers. To separate these two pathways, we fabricate EML composite films, HODs, and EODs. To investigate the degradation by excited-state stress, we measured the change in photoluminescence (PL) internsity / initial PL intensity (PL/PL_0) of the composite films under continuous excitation light illumination. The used excitation light had 375 nm of wavelength with 16 mW power. The Figure 4.5 exhibited the PL/PL_0 curves of the composite films. The all curves show steep decrease in short time period and the gradient became more gradual in long time period. It is obvious that the composite films with mixed host significantly have improved stability, especially mCP : DPEPO 1: 1 mixture host film exhibited the best stability. Though the mCP host film shows better stability compared to that of DPEPO, the OLED with mCP as host has poor lifetime due to its bad EL performance with high driving current.

To obtain further insight into the EML degradation, we fabricated HODs and EODs to investigate the electrochemical stabilities to the electrons and holes. The PL/PL_0 curves of the EODs and HODs are shown in Figure 4.6. The all single carrier devices were continuously biased at 5.1 mA/cm^2 which was similar current density of 500 cd/m^2 driving for blue OLEDs with no light illumination, and the PL intensities of the single carrier devices were measured after the constant-current operation was stopped. The PL/PL_0 curves of single carrier devices show small degradation compared to those of composite films. However, it was hard to find the

similar trends with degradation of composite films and OLEDs. We could presume that the decrease in PL/PL_0 in HODs and EODs is caused by electrochemical instability of radical cations and anions after migration of unwanted chemical species []. In addition, it was confirmed that the deterioration of charge transport and injection to EML inside the OLEDs act as the one of reasons on L/L_0 decrease in blue OLEDs. We could expect this explanation by driving voltage increases in single carrier device during constant-current bias as shown in Figure 4.7.

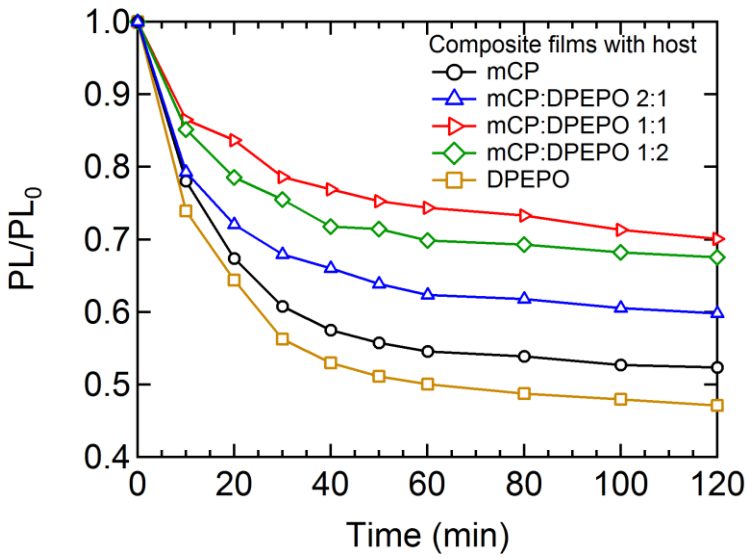

Figure 4.5 Changes in PL/PL_0 of the EML composite films as a function of operational time.

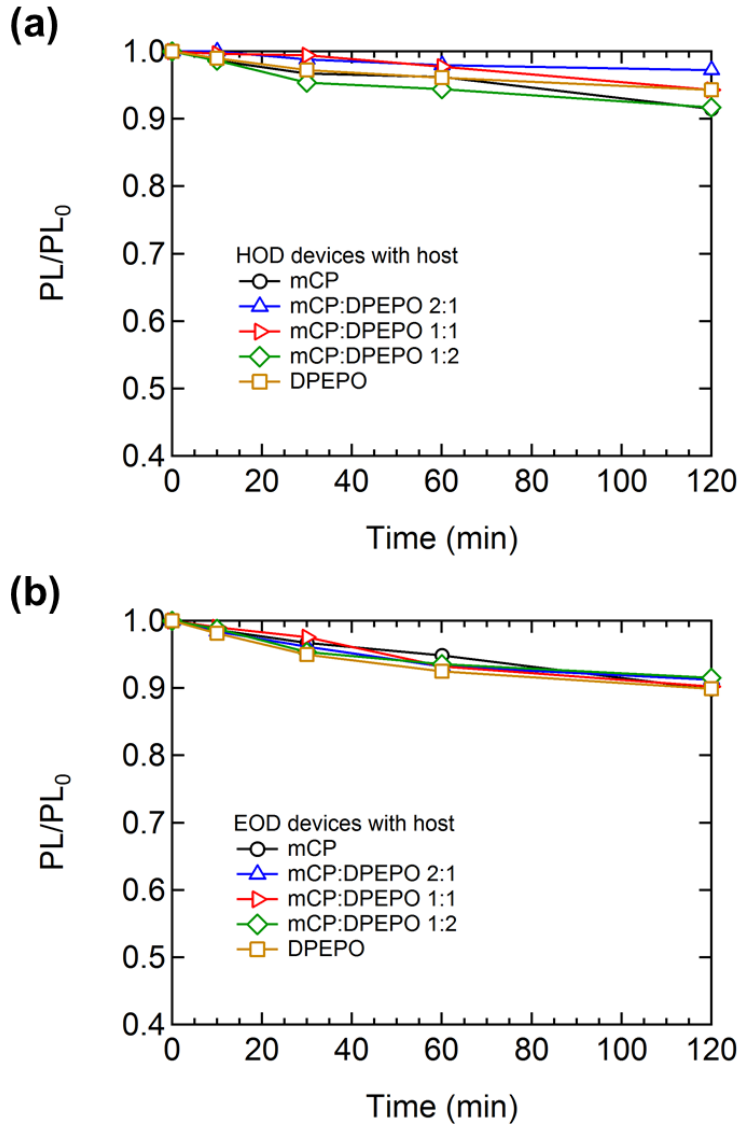

Figure 4.6 Changes in *PL/PL$_0$* of (a) HODs, and (b) EODs under continuous constant-current bias as a function of operational time.

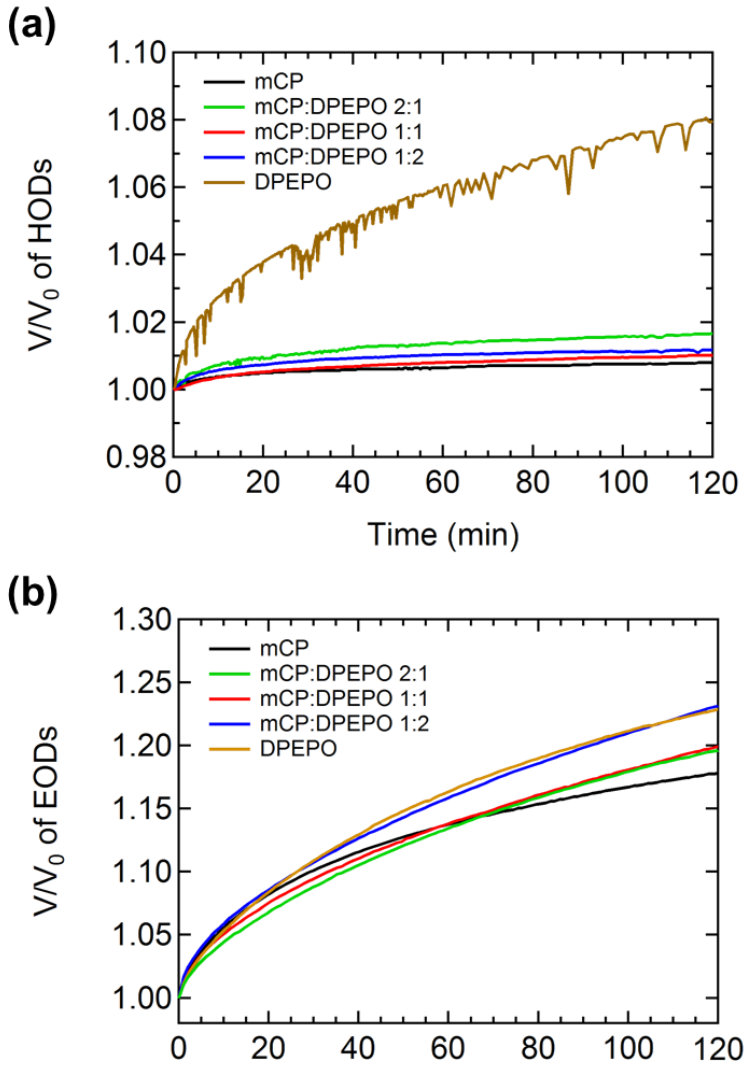

Figure 4.7 Changes in V/V_0 of (a) HODs, and (b) EODs under constant-current bias as a function of operational time.

Figure 4.8 displays the changes in luminance/initial luminance (L/L_0) of OLED and PL/PL_0 of composite films, HODs, and EODs simultaneously. The PL/PL_0 curve of the composite film almost agrees with the L/L_0 curve of the OLED over a short time period, indicating that the OLED degradation mainly occurs because of the excited-state instability of EML. In addition to the decrease in L/L_0 of OLEDs, it was confirmed that the degradation by charge carriers affected small portion. Also the reduced carrier injection and transport might be expected to induce an imbalance in the numbers of holes and electrons in the EMLs as we discussed with Figure 4.7. It is obvious that the stability of excited-state stress improvement by mixed host contributed to the OLED lifetime enhancement. Actually, we could not specify the reason of this trend, but we speculate that the mixing of two molecules reduced the intermolecular interaction between mCP and DMAC-DPS, and suppressed the excited state of DMAC-DPS and DPEPO reaction by dispersion of mCP molecules.

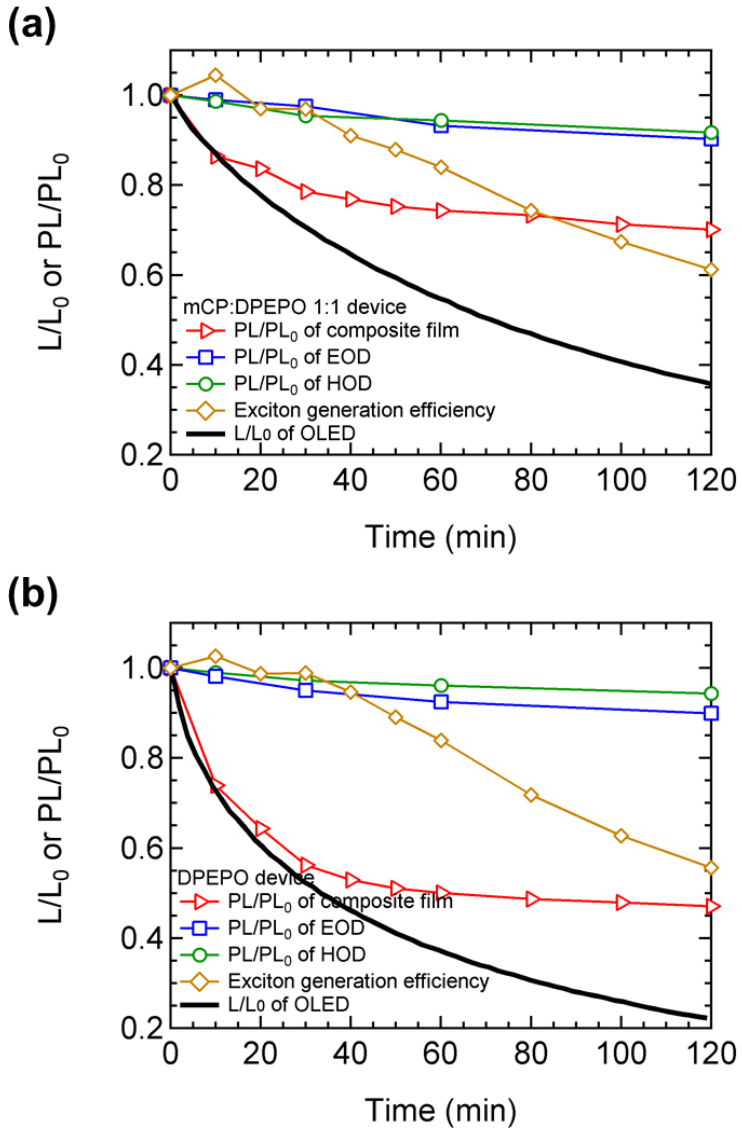

Figure 4.8 Summarized changes in L/L0 of the OLEDs and PL/PL0 of the composite films, EODs, and HODs of (a) device with mCP:DPEPO 1:1 as host, and (b) DPEPO as host.

The decreases in L/L_0 and PL/PL_0 can be attributed to two mechanisms. In first mechanism, the degradation products, generated during OLED operation, act as exciton quenchers [70]. In this case, the macroscopic PL quantum yield can be effectively reduced by the small number of exciton quenchers. In second mechanism, the degradation products themselves are not luminescent but do not act as exciton quenchers (non-radiative recombination centers). To identify the formation of exciton quenchers in the degraded OLEDs, the transient EL technique was used.

Figure 4.9 shows the TREL profiles of pristine and degraded OLEDs. In all devices, the TREL curves of degraded OLEDs decay more quickly than that of the pristine devices, indicating the formation of exciton quenchers during OLED operation. Table 4.2 summarized the decay time of delayed component of all results.

Table 4.2 Summarized parameters of transient EL decay curves of fabricated blue TADF OLEDs with different host structures.

	mCP		mCP:DPEPO 2:1		mCP:DPEPO 1:1		mCP:DPEPO 1:2		DPEPO	
	Pristine	Degrad	Pristine	Degrad	Pristine	Degrad	Pristine	Degrad	Pristine	Degrad
A_1	0.49	0.43	0.50	0.46	0.50	0.47	0.44	0.44	0.42	0.42
τ_1	1.92 μs	1.36 μs	2.47 μs	1.82 μs	2.51 μs	1.90 μs	2.54 μs	1.97 μs	2.61 μs	1.90 μs
A_2	0.29	0.31	0.29	0.29	0.33	0.32	0.37	0.34	0.37	0.35
τ_2	6.88 μs	4.72 μs	8.45 μs	7.01 μs	8.54 μs	7.54 μs	9.04 μs	8.15 μs	10.8 μs	9.33 μs

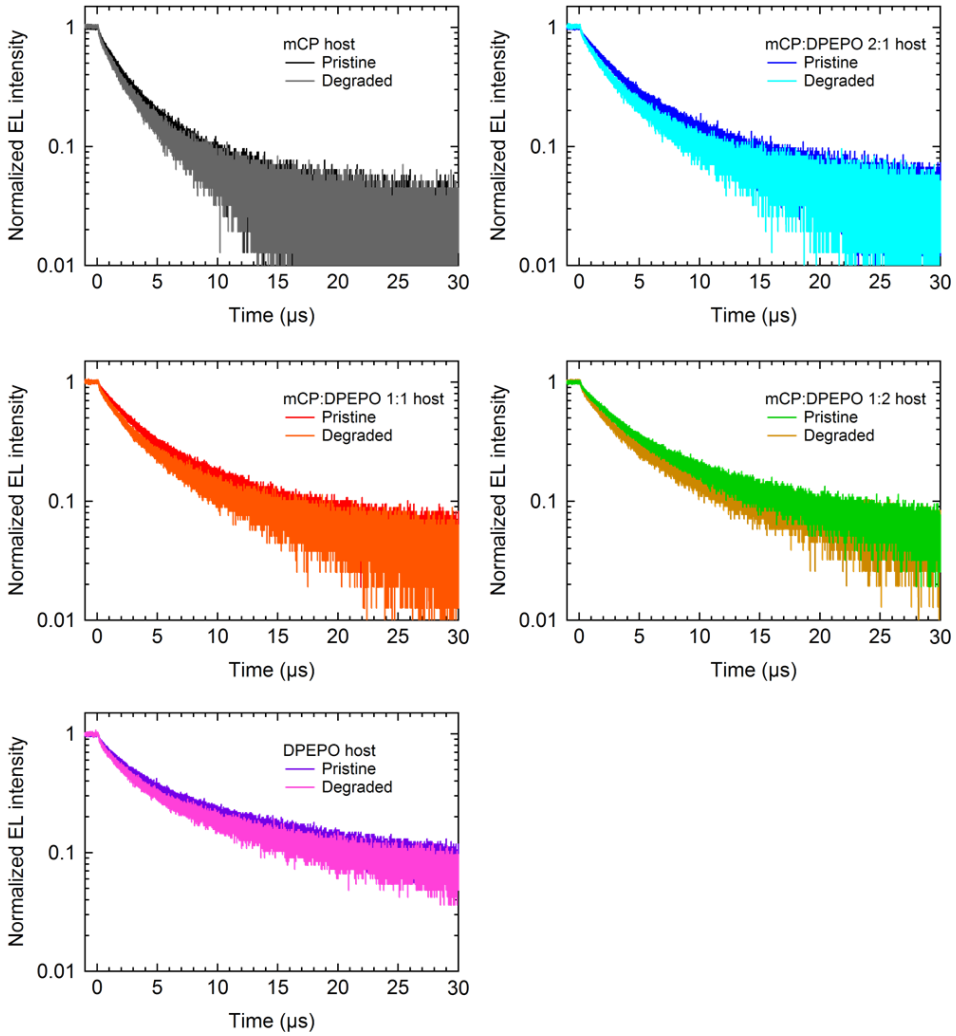

Figure 4.9 Transient EL decay curves of fabricated blue TADF OLEDs with different host structures.

4.3 Appendix

If the macroscopic degradation of device is severe, the analysis of above experiment cannot be persuasive. To elucidate this problem, we also investigate the macroscopic images of device pixels. As shown in Figure 4.10, there are some dark spots on the pixels. However, we can find that it is not major degradation reason such as electrode detachment.

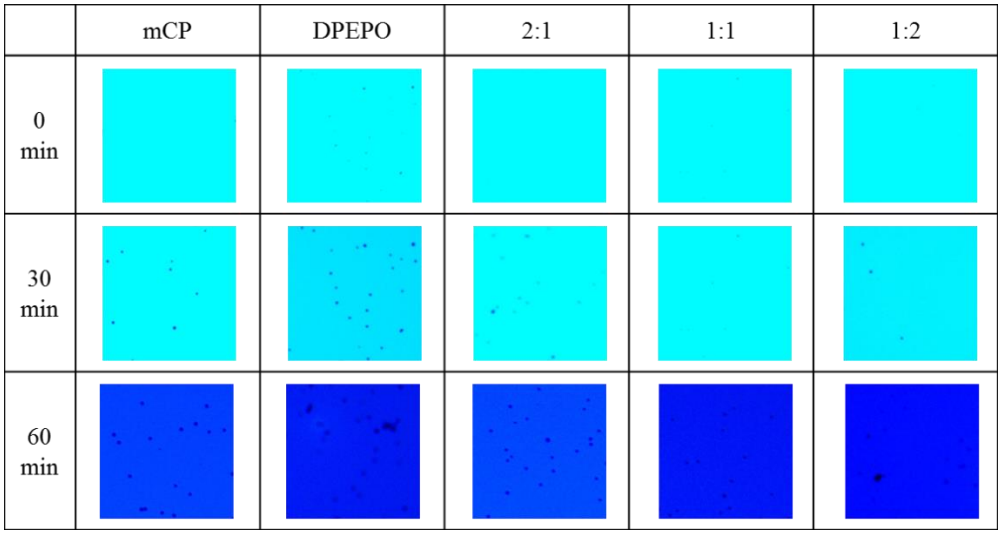

Figure 4.10 The optical microscopy images of fabricated pixels.

4.4 Summary

In summary, we investigated the mechanisms of degradation on blue OLEDs based on TADF emitter. The mixed host using mCP and DPEPO clearly reduced the excited-state instability resulting in enhancement of device lifetime. The blue OLED with host 1 : 1 mCP : DPEPO shows enhanced LT50 of 61.4 min compared to the device with DPEPO as host having LT50 of 35.5 min. In terms of the device efficiency, the devices with higher DPEPO concentration show higher values. The blue OLED with DPEPO host exhibited 21.4 % maximum EQE, which is higher than that of the device with 1 : 1 mCP : DPEPO as host of 20.0 %. Also the mixed host improves the efficiency roll-off properties. To prove the degradation mechanisms of blue OLEDs based on TADF emitter, we fabricated EML composite films, HODs, and EODs and measured the PL degradation. The EML composite films under continuous excitation light illumination show the degradation patterns similar with those of OLED devices. It is obvious that mixed host enhanced the excited-state stability. The short device lifetime of mCP was due to its low EL performance. Meanwhile, the PL degradations with continuous constant-current bias in HODs and EODs were very small compared to the composite films, indicating that excited-state instability is main cause of short-time period degradation of OLEDs and deterioration of charge carrier transport is the cause of long-time period degradation. We also demonstrated that the degradation product can act as exciton quencher. We believe that the results will contribute to the develop of high stability blue OLEDs based on TADF emitters.

Chapter 5

Enhanced Stability of Hybrid White OLEDs based on TADF Blue Emitter Using Mixed Host Systems

As well known, in blue fluorescent EML in the multi-EML hybrid white OLEDs, the singlet excitons of only 25 % can be utilized for the blue emission, while the triplet excitons of 75 % are generally diffused to the adjacent phosphorescent layer, termed as 'triplet harvesting' strategy, to fully utilized all excitons. However, the absence of blue fluorophores with high triplet energy level (T_1) and photoluminescence quantum yield (PLQY) greatly limits the performance of multi-EML hybrid white OLEDs, where the reverse energy transfer from the phosphorescent emitters to the low-lying triplet state of fluorescent emitters, which significantly quenches the triplet excitons [35,51,72]. Since, the utilization of more efficient blue fluorescent

emitters with high T_1 and PLQY is obviously imperative for the development of high-performance hybrid white OLEDs.

Recently, a remarkable breakthrough on the development of thermally activated delayed fluorescence (TADF) materials by Adachi and co-workers makes the more efficient blue fluorophores with high T_1 feasible [59]. Due to the generated triplet excitons can be used by a reverse intersystem crossing (RISC) process induced by very small singlet-triplet energy gap, thus the TADF materials can achieve 100 % exciton utilization efficiency as the alternative of phosphors. Nowadays, the highly efficient blue TADF materials with high T_1 and PLQY have been successfully synthesized [69], As shown, although some TADF-based hybrid WOLEDs have achieved an impressive electroluminescence (EL) efficiency, the problems are still obvious in terms of severe efficiency roll-off, poor color stability, poor device stability [73-76]. The realization of high efficiency, superior color stability, good stability, and low efficiency roll-off simultaneously in TADF-based hybrid white OLEDs remains a big challenge.

In this section, we demonstrated high-performance TADF-based hybrid white OLEDs employing efficient TADF material as the blue emitter, combined with mixed host systems.

5.1 Hybrid white OLEDs based on TADF blue emitter without mixed host system

To demonstrate the viability of TADF blue emitter for high-performance hybrid white OLEDs, we firstly fabricated the fluorescence / phosphorescence hybrid white OLEDs based on DMAC-DPS as TADF blue emitter. For yellow phosphorescent emitter, PO-01 was used. TCTA served as phosphorescent host and DPEPO was used as host of DMAC-DPS TADF blue emitter due to high triplet energy level of DPEPO (3.3 eV) and high PLQY (90 %) of DMAC-DPS doped film [69]. Figure 5.1 shows the proposed energy level diagram of the EML of fabricated hybrid white OLEDs.

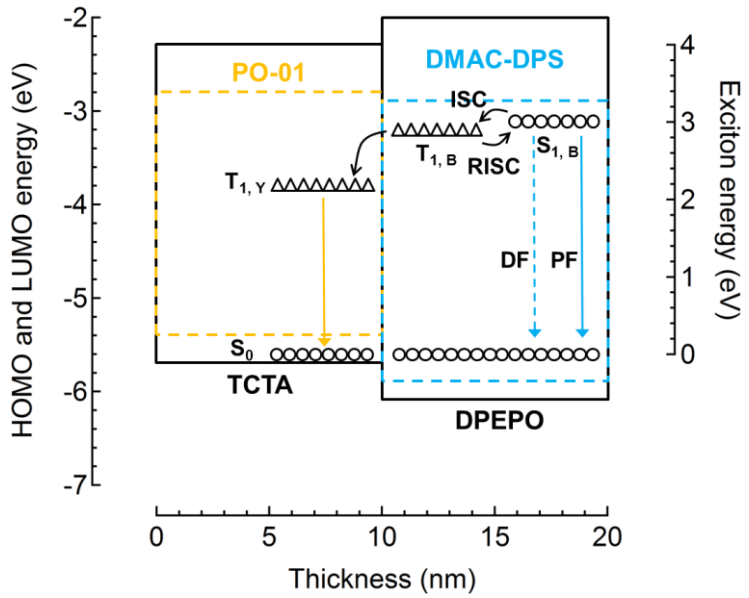

Figure 5.1 The energy level diagram of emitting layer of hybrid WOLED. Solid lines and dashed lines refer to HOMO and LUMO energy levels. Circles and triangles correspond to the exciton energies.

The structure consist of ITO / MoO_3 (10 nm) / TAPC (50 nm) / TCTA:PO-01 (8 wt%, 10 nm) / DPEPO:DMAC-DPS (10 %, 8 nm) / TmPyPB (30 nm) / LiF / Al. As shown in Figure 5.2, the proposed hybrid white OLED shows excellent EL performances. The maximum EQE, CE, and PE are 21.7 %, 50.0 cd/A, and 48.9 lm/W, respectively, which are even comparable to those of the state-of-the-art all phosphorescent white OLEDs. At the practical luminance 1000 cd/m^2, they still remain as high as 16.4 %, 35.0 cd/A, and 23.8 lm/W, exhibiting less pronounced efficiency roll-off compared to other TADF based white OLEDs. (However, it still very bad performance due to the high current density luminance roll-off in blue EML with DPEPO host. (See **Section 4**) **Table 5.1** summarizes the EL performances of the representative white OLEDs in previous studies. All the results were obtained in the normal direction without any outcoupling enhancement techniques. Also, when the luminance changes from driving current density 1.28 mA/cm^2 to 25.5 mA/cm^2 matched with 560 to 6700 cd/m^2, the EL spectra of this device turn out to be rather stable, and the changes of CIE coordinates is small (< 0.01, 0.01). In general, various colors-based white OLEDs have large color shift due to the exciton recombination zone changes as the driving current density increases. However, the stable exciton generation zone at the interface of blue and yellow EML in our device contributed to the color stability.

Table 5.1 Comparison of the device performances for the representative WOLEDs.

	Type	EQE max	EQE 1000 cd/m^2	PE max	PE 1000 cd/m^2	CIE
[77]	All phosphor	19.0 %	15.9 %	52.7 lm/W	33.2 lm/W	(0.34, 0.35)
	All phosphor	21.6 %	21.5 %	59.9 lm/W	43.3 lm/W	(0.40, 0.40)
[78]	All phosphor	19.3 %	-	42.5 lm/W	-	(0.33, 0.39)
[79]	All phosphor	22.4 %	22.0 %	46.6 lm/W	41.3 lm/W	(0.45, 0.45)
[55]	Hybrid	16.3 %	-	41.0 lm/W	-	(0.38, 0.46)
[80]	Hybrid	21.2 %	20.0 %	40.7 lm/W	37.1 lm/W	(0.42, 0.44)
[73]	Hybrid TADF	22.9 %	-	-	-	(0.31, 0.33)
[74]	Hybrid TADF	25.5 %	14.8 %	84.1 lm/W	24.2 lm/W	(0.40, 0.43)
[75]	Hybrid TADF	19.6 %	13.6 %	50.2 lm/W	-	(0.42, 0.48)
[76]	Hybrid TADF	23.0 %	17.5 %	51.7 lm/W	19.5 lm/W	(0.44, 0.44)
This work	**Hybrid TADF**	**22.1 %**	**18.0 %**	**50.3 lm/W**	**26.6 lm/W**	**(0.42, 0.42)**

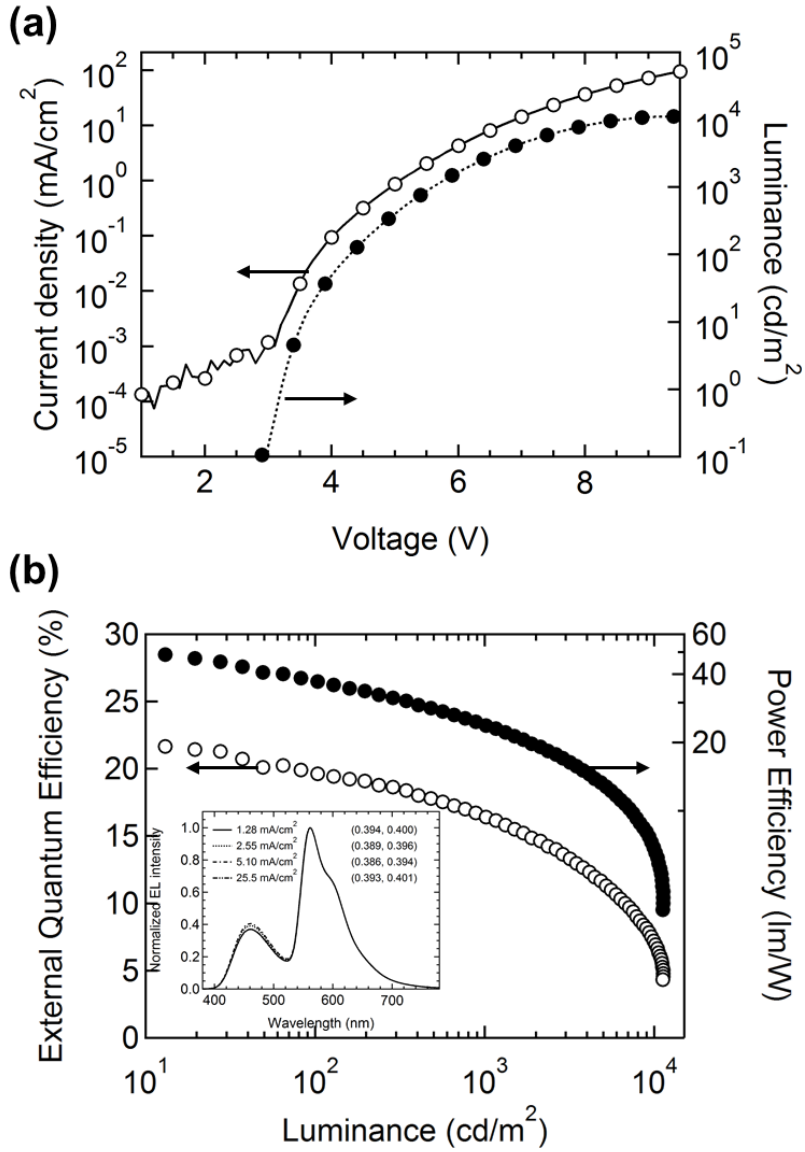

Figure 5.2 (a) Current density-voltage-luminance characteristics of white device, and (b) external quantum efficiency and power efficiency versus luminance characteristics of white device. The inset represents the normalized EL spectra at different driving current density.

In order to elucidate that where is the origin of blue emission and yellow emission, time-resolve transient EL decay curves were measured. If the blue emission arises from DMAC-DPS TADF blue emitter, the delayed component should be detected. As shown in Figure 5.3, we could find the delayed decay component in transient EL curve of white device measured at 460 nm wavelength. The decay time was 4.5 μs which is clearly originated from TADF emitter. The transient decay of phosphorescence emission generally has 1 microsecond decay time. However, the measured transient decay at 560 nm wavelength shows a microsecond-scale delayed part, which is an intrinsic characteristic of the TADF process [81]. To prove that it really comes from DMAC-DPS TADF emitter, we fabricated other device having same structure of white device except nonexistence of DMAC-DPS. Obviously, a delayed component in the white device was observed, while it was not observed in the device without DMAC-DPS TADF blue emitter. The transient decay time of the delayed component is dependent on that of DMAC-DPS emitters in the hybrid white OLEDs. The measured decay time was ~3.1 μs and it was well matched with the decay time of DMAC-DPS emitter [69], which indicates that the excitons originating from the DMAC-DPS blue emitter is being transferred to PO-01 molecules in the hybrid white OLEDs.

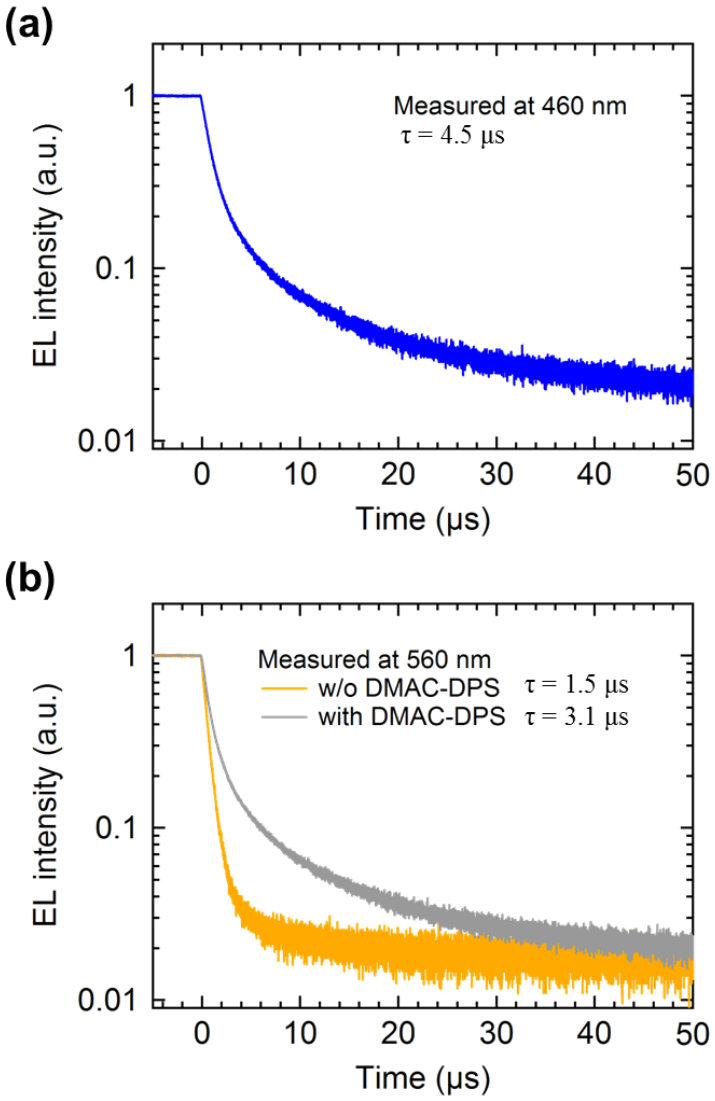

Figure 5.3 Time-resolved EL decay curves of (a) white device measured at 460 nm wavelength, and (b) white device and device without DMAC-DPS measured at 560 nm wavelength.

As we can see the results (See Figure 5.4), the yellow phosphorescent emitter concentration affects to the emission spectrum by influencing the probability of energy transfer from DMAC-DPS molecules to yellow phosphor. We decreased the PO-01 doping concentration from 8 % to 2 %. The results show different EL spectra with CIE coordinates (0.35, 0.37) for 4 %, and (0.32, 0.35) for 2 %. Due to the low probability of exciton energy transfer from DMAC-DPS to PO-01 in low doping concentration device, the blue emission was increased and PEs were decreased to 34.5 lm/W for 2 % doping concentration.

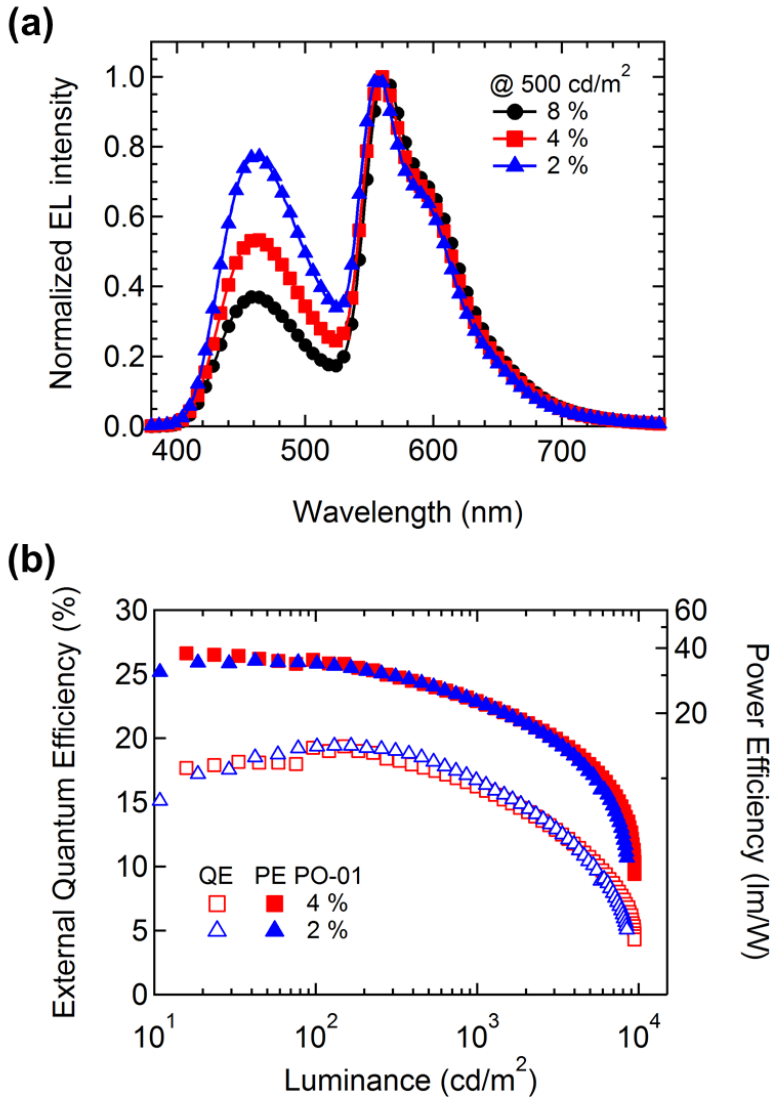

Figure 5.4 (a) Normalized EL spectra, and (b) EQE and PE versus luminance of white devices with different yellow phosphor doping concentration.

5.2 The stability issues in TADF based hybrid WOLEDs

We also measured the device lifetime of fabricated hybrid WOLEDs. The initial measured luminance was 3000 cd/m^2. Figure 5.5 displays the device lifetime of hybrid WOLED and EL spectrum change with degradation. Although our device has excellent EL performance, the operational stability was very poor (LT50 ~ 1 h). It is obvious that the blue emission stability was very poor. Many groups pointed out the DPEPO host should be one of the reasons for the poor lifetime and mainly host stability affects to the TADF based device lifetime.

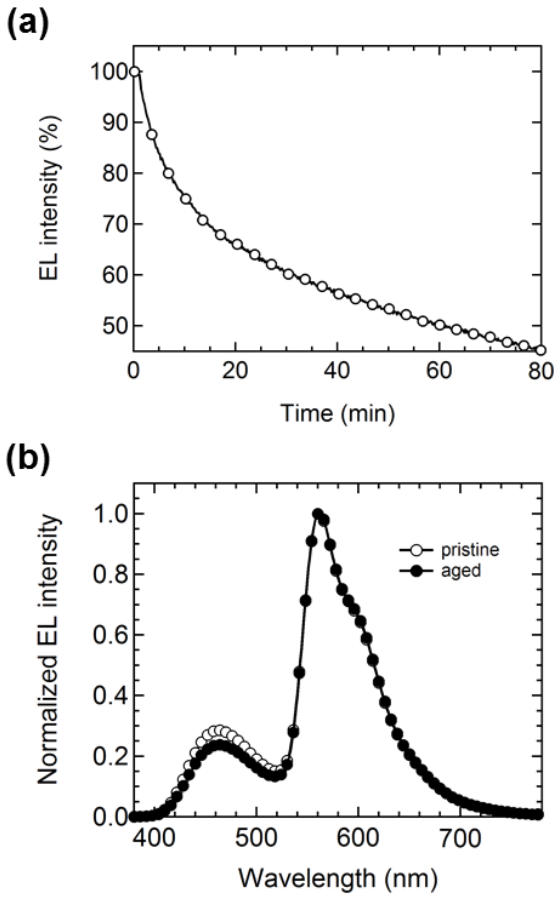

Figure 5.5 (a) The lifetime of WOLED in this section, and (b) normalized EL spectrum change with degradation.

5.3 Hybrid white OLEDs based on TADF blue emitter with mixed host system

In **Section 4**, we demonstrated the effect of mixed host on DMAC-DPS based TADF blue OLEDs. The results gave us the insight that the 1 : 1 mixing ratio of mCP : DPEPO mixed host layer exhibited enhanced device stability due to its reduced excited-state instability. Also the blue OLED device with mixed host exhibited low efficiency roll-off and high current density luminance roll-off. With the result of hybrid WOLED discussed in previous section, we expected that the mixed host in blue EML based on TADF emitter could also enhance the device performance and stability of hybrid WOLEDs.

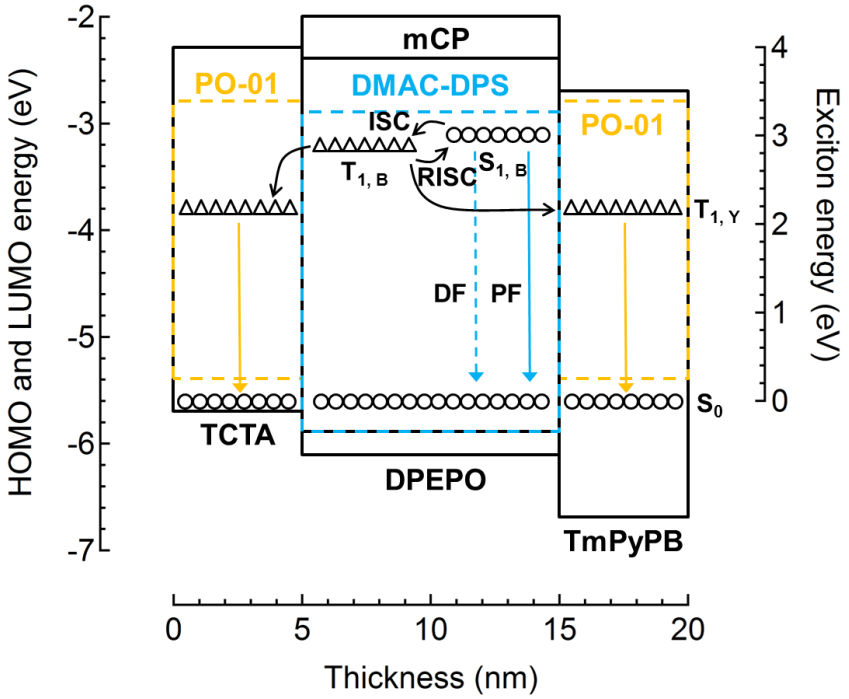

Figure 5.6 The schematic diagram of emitting layer of fabricate device in this section. Circles show single exciton energy level and triangles show triplet exciton energy level.

Figure 5.6 shows the structure of EML on this section. First, we adopted the mixed host of mCP and DPEPO with mixing ratio of 1 : 1 for blue EML with DMAC-DPS as TADF emitter. Then, we constructed the yellow EML on both sides of blue EML in order to elucidate the exciton generation zone position. To construct yellow EML on both sides, the hole transporting TCTA and electron transporting TmPyPB served as host of the yellow phosphorescent emitter of PO-01. The detailed structures of EMLs are described below.

Device A : TCTA:PO-01 (8 wt%, 5 nm) / mCP:DPEPO:DMAC-DPS (1:1, 10 %, 10 nm) / TmPyPB (5 nm)

Device B : TCTA (5 nm) / mCP:DPEPO:DMAC-DPS (1:1, 10 %, 10 nm) / TmPyPB:PO-01 (8 wt%, 5 nm)

Device C : TCTA:PO-01 (8 wt%, 5 nm) / mCP:DPEPO:DMAC-DPS (1:1, 10 %, 10 nm) / TmPyPB:PO-01 (8 wt%, 5 nm)

Table 5.2 Summary of the performance of fabricated white devices. *Critical current density, where EQE declines by half from its maximum, **driving current density from 2.55 mA/cm^2 to 25.5 mA/cm^2.

Device	Max. E.Q.E.	E.Q.E. @1000 cd/m^2	Max. P.E.	P.E. @1000 cd/m^2	J_c*	(Δx, Δy)**
Device A	19.1 %	13.8 %	41.2 lm/W	19.5 lm/W	26.5 mA/cm^2	< (0.02, 0.02)
Device B	20.8 %	17.3 %	48.4 lm/W	26.4 lm/W	42.0 mA/cm^2	< (0.01, 0.01)
Device C	22.1 %	18.0 %	50.3 lm/W	26.6 lm/W	64.5 mA/cm^2	< (0.003, 0.003)

Figure 5.7 exhibited the current density-voltage and luminance-voltage characteristics of fabricated devices. As we can see, the current densities of device A and C are lower than that of device B due to the hole trap property of PO-01 doping on the TCTA hole transporting host. The luminance of device B is much higher than that of device A, indicating the more exciton is quenched through TCTA compared to TmPyPB. In device B, the luminance roll-off in high current density is severe because of exciton accumulation in the interface of blue EML and yellow EML on TmPyPB. Conversely, the device A and C have lower luminance roll-off in high current density due to the hole trap of yellow EML on TCTA, which is beneficial to broaden exciton recombination zone and suppress the exciton accumulation. The detailed performance parameters are summarized on Table 5.2

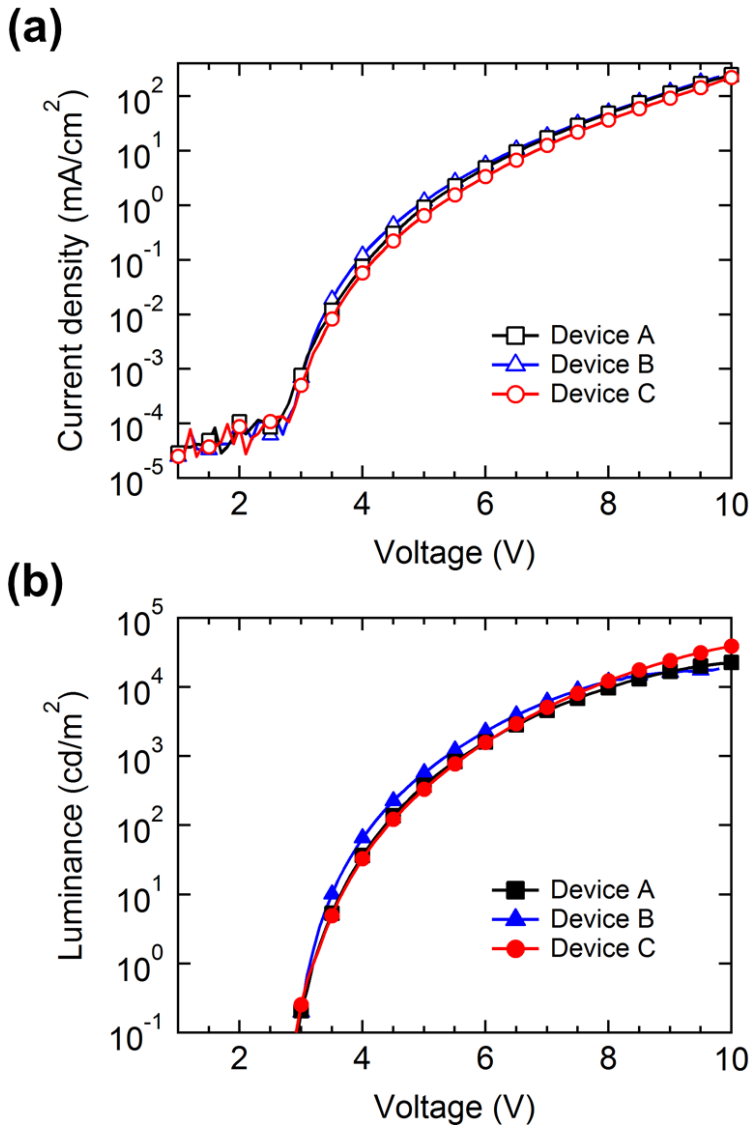

Figure 5.7 (a) Current density-voltage (J-V) characteristics and (b) luminance-voltage (L-V) characteristics of fabricated hybrid WOLEDs.

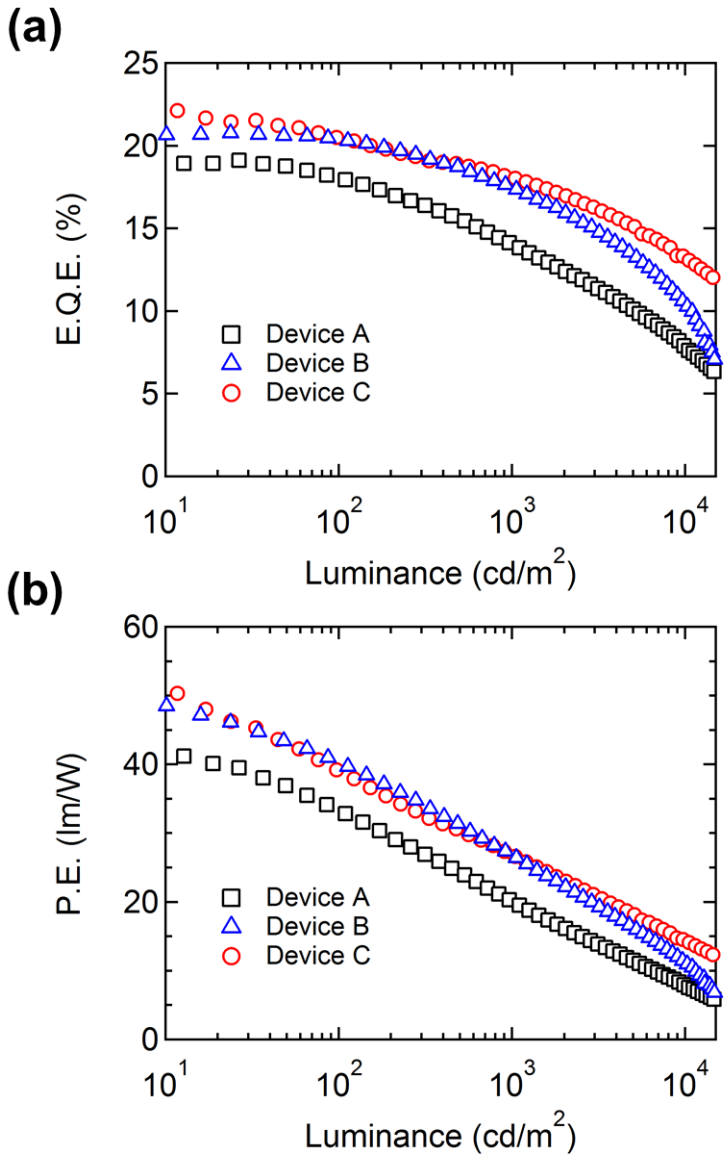

Figure 5.8 (a) External quantum efficiency and (b) power efficiency versus luminance of fabricated hybrid WOLEDs

Figure 5.8 displays the EQE and PE characteristics versus luminance. The maximum EQEs of device A, B, and C were 19.1, 20.8, and 22.1 %, respectively. The maximum PEs of device A, B, and C were 41.2, 48.4, and 50.3 lm/W, respectively. At the practical brightness of 1000 cd/m^2, they were 13.8, 17.3, and 18.0 % of EQE and 19.5, 26.4, and 26.6 lm/W, respectively. The device C has very low efficiency roll-off property. Figure 5.9 exhibited the normalized EL spectra of fabricated devices at different driving current densities. The results support the exciton generation zone and exciton quenching processes. The spectrum of device B has stronger yellow emission compared to that of device A, indicating the main exciton generation zone is located slightly at ETL side of blue EML. In the device A, the spectral changes with increasing current density which have increased blue emission and decreased yellow emission mean that the exciton generation zone shift to ETL side which is far away from yellow emitters with increasing current density. This hypothesis also coincides with the results of device B. The decreased exciton quenching through TCTA layer is the cause of blue emission increase. On the other hand, the device C exhibited very stable color coordinate due to the yellow EML on both sides compensate the change of main exciton generation zone shift. The low efficiency roll-off of device C is caused by no exciton quenching site on both sides.

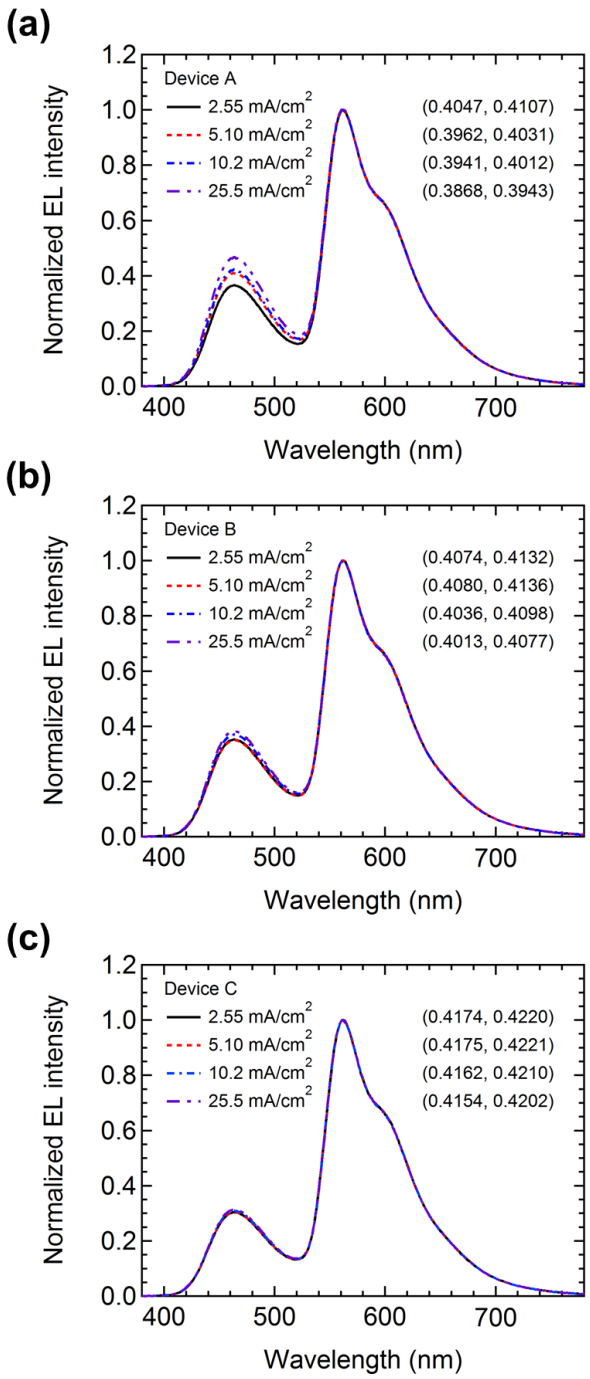

Figure 5.9 The normalized EL spectra of (a) device A, (b) device B, and (c) device C with respect to the different current density.

To support the exciton harvesting mechanism and exciton generation zone distribution hypothesis, we also measured the time-resolved EL decay curves of fabricated WOLEDs. The measurement was achieved on yellow emission of wavelength 560 nm. In **Section 4.2**, we addressed that the existence of exciton quencher effectively reduced the PL quantum yield and the decay time of emission is being shorter. As shown in Figure 5.10, all devices exhibited different decay time components. We fitted the curves using double exponential function. The first decay component is corresponding to emission with direct exciton recombination on yellow phosphor, and second decay component is corresponding to delayed emission due to the excitons transferred from DMAC-DPS molecules. The fitted components are described in Table 5.3. All three devices were fitted direct decay time constant ~ 0.8 μs and delayed decay time constant ~ 3.0 μs. The device B exhibited much larger portion of delayed component compared to device A because main exciton generation zone is located close to ETL side. Also the large portion of direct recombination in device A comes from charge trap assisted self-emission in yellow phosphor. Moreover, the small amount of delayed component in device C elucidate that direct emission by charge trap on yellow phosphor in TCTA host broadens exciton generation zone and suppress exciton accumulation at the interface of blue EML and TmPyPB layer.

As shown in Figure 5.11, we could find that the delayed component in WOLEDs came from the excitons transferred from DMAC-DPS. The device without DMAC-DPS only exhibited direct recombination component with the decay time 0.8 μs.

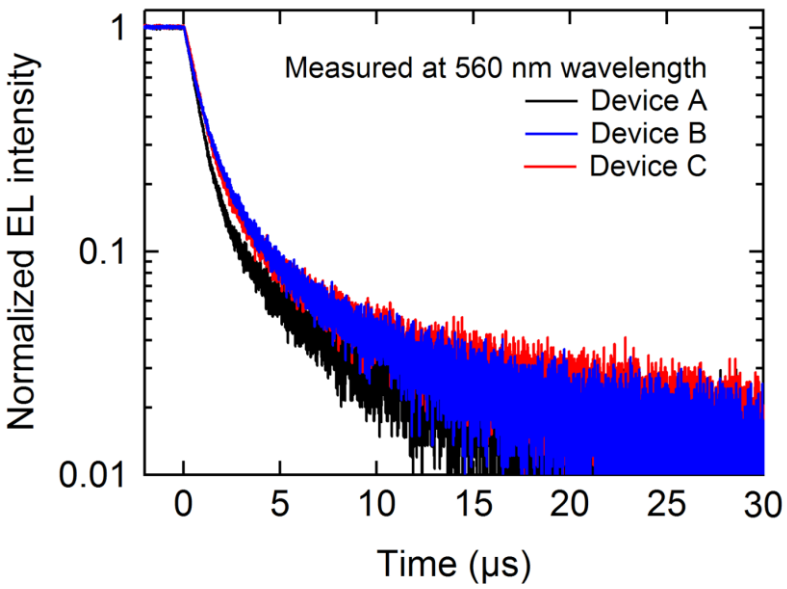

Figure 5.10 The transient EL decay curves of fabricated WOLEDs based on mixed host.

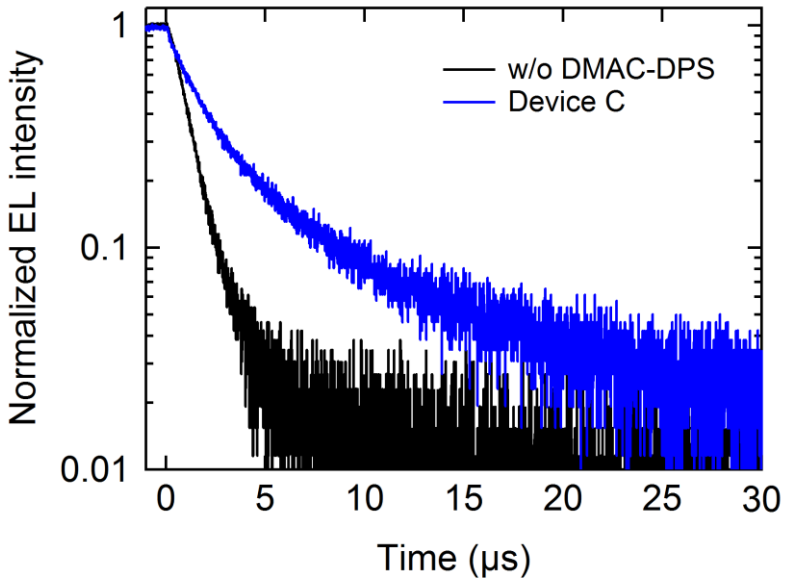

Figure 5.11 The transient EL decay curves of the devices with and without DMAC-DPS.

Table 5.3 Summary of fitted parameters for transient decay curves.

	Device A		Device B		Device C	
τ_1 , A1	0.8 μs	0.80 ± 0.001	0.8 μs	0.62 ± 0.001	0.8 μs	0.72 ± 0.001
τ_2 , A2	3.0 μs	0.14 ± 0.001	3.0 μs	0.31 ± 0.001	3.0 μs	0.20 ± 0.001

Table 5.4 Summary of efficiency roll-off and device lifetime trends.

	Device A	Device B	Device C	w/o mixed host
LT50	77.5 min	100.2 min	143.6 min	60.6 min
$J_{1/2EQE}$	26.5 mA/cm^2	42.0 mA/cm^2	64.5 mA/cm^2	21.5 mA/cm^2

5.4 The stability of hybrid WOLEDs with mixed host

The device lifetimes of hybrid WOLEDs discussed in this section were also measured. The initial luminance of measurement was 3000 cd/m^2. Figure 5.11 shows the device lifetime curves and EQE curves of fabricated devices. The result which was discussed in **Section 5.1** also compared simultaneously. As a result, the device C shows the best stability properties with LT50 of 143.6 min. The LT50 of device A and B were 77.5 min and 100.2 min, respectively. Due to the exciton quenching processes in device A and B, the efficiencies and lifetimes of the devices are worse compared to device C. The device discussed in previous section shows much lower stability due to the low blue EML stability (see **Section 4**), indicating that the mixed host in blue EML is superior technique for enhancing the device stability.

Efficiency roll-off properties trend correspond to the device stability trend. The detailed parameters are summarized in Table 5.4. The higher critical current density, where EQE declines by half from its maximum, the higher device stability was observed. It coincides with the results of **Section 3**. The device C shows the good J_c of 64.5 mA/cm^2. All other devices have lower values than device C. Especially, it was much higher than that of the device without mixed host which have J_c of 21.5 mA/cm^2. Although it still lower than common hybrid WOLEDs reported before, it is superior result compared to other reported hybrid WOLEDs based on TADF blue emitters as described in Table 5.1. However, the lifetime of hybrid WOLEDs based on TADF blue emitter still lower than that of **Section 3**. It is because the stability of TADF blue emitter is still low, the longest lifetime of TADF blue emitter reported is about 420 hours [82]. Also the results of this thesis are the best lifetime reported in journal papers as our knowledge.

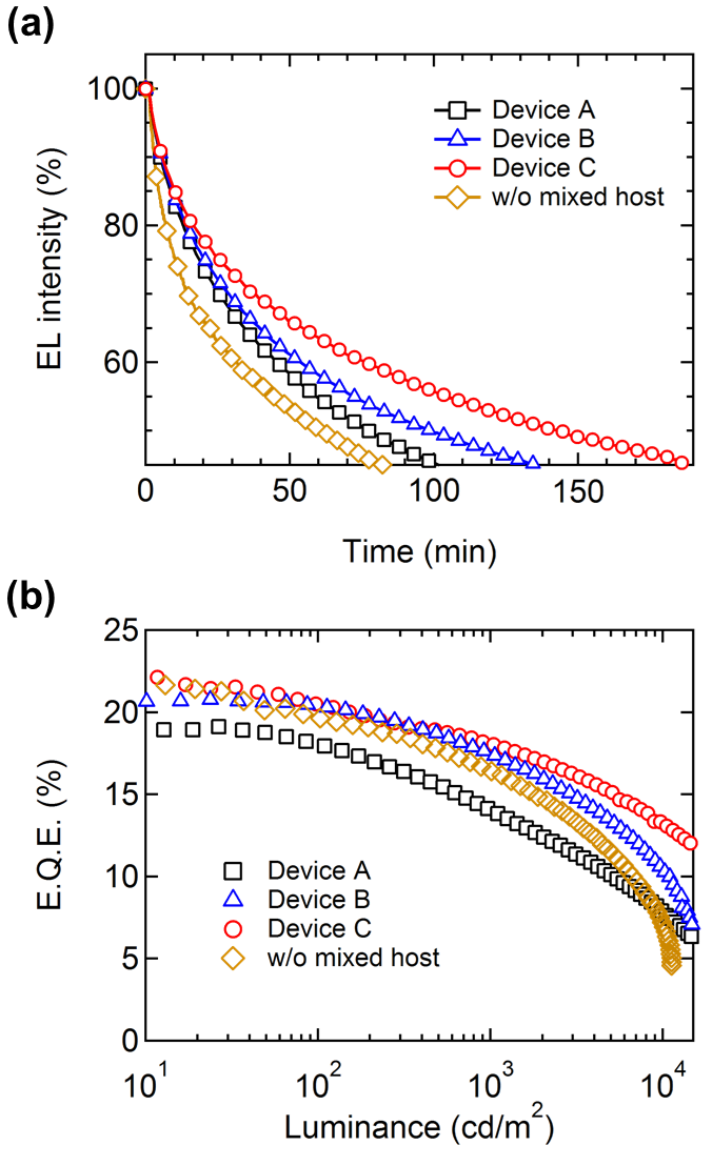

Figure 5.12 (a) Device lifetime curves and (b) EQE versus luminance of fabricated WOLEDs. The device without mixed host system exhibited short device lifetime and large efficiency roll-off.

5.5 Summary

We demonstrated that high-performance hybrid WOLEDs with superior color stability, low efficiency roll-off, and device stability. The presented approach to significantly boost the device stability was mixed host system on blue EML based on TADF emitter. Also the structure with two yellow EML positioned in the side of blue EML gave the color stability regardless of exciton generation zone shift. The comprehensive experiment like transient EL measurement and device spectrum shift measurement elucidate the exciton generation zone position and shift characteristics. The proposed device exhibited superior maximum external quantum efficiency, current efficiency, and power efficiency of 22.1 %, 59.3 cd/A, and 50.3 lm/W, respectively. Moreover, the device exhibited color stability with small CIE coordinate shift of (< 0.003, 0.003). Although the severe efficiency roll-off is general problem of hybrid WOLEDs based on TADF emitter, our device with mixed host on blue EML has high critical current density of 64.5 mA/cm^2. Other important feature of proposed device is improved device lifetime. The hybrid WOLED without mixed host system exhibited LT50 ~ 1h. We demonstrated that the proposed device shows LT50 ~ 2h which was two times longer result. We expect that this result provide the designing key point for further research towards high-performance and stable hybrid WOLEDs based on TADF emitters.

Chapter 6

Conclusion

In this thesis, we investigate the mixed host system for high-performance hybrid WOLEDs and device stability of blue OLEDs based on TADF emitter. The efficient hybrid WOLEDs with general blue fluorophore and TADF emitter were demonstrated.

First, we demonstrated the device design strategy for non-interlayer hybrid WOLEDs. The mixed host for blue EML which manipulates exciton generation zone and suppressed the unwanted exciton energy transfer was major feature in this device. The developed device exhibited enhanced performance of 17.1 % maximum EQE, and 36.0 lm/W maximum PE. However, demonstrated non-interlayer device shows poor lifetime compared to interlayer device due to inevitable exciton quenching between blue and yellow EML, confirming that blue fluorophore with high triplet energy level is needed for further improving of device efficiency and lifetime.

Second, the degradation mechanism of blue OLEDs based on TADF emitter was investigated and proposed the mixed host for solution of enhancing device lifetime. As a result, the excited-state instability of host material is the main cause of OLED degradation. Moreover, the electrochemical instability forming non-radiative recombination centers and inducing charge imbalance brings about OLED degradation at long term period. Also, it is found that the degradation products act as exciton quenchers. The proposed mixed host system on blue EML improves the stability on excited-state stress and broadens the exciton generation zone. Especially, the device having 1 : 1 mixing ratio host exhibited 2 times longer lifetime compared to the device with DPEPO host.

Finally, we developed high-performance hybrid WOLEDs with superior efficiency, color stability, low efficiency roll-off, and better lifetime based on blue TADF emitter. The resulting WOLED shows the maximum external quantum efficiency, current efficiency, and power efficiency of 22.1 %, 59.3 cd/A, and 50.3 lm/W, respectively. Moreover, the device exhibits extremely stable EL spectra with Commision Internationale de L'Eclairage (CIE) coordinates of (0.417, 0.422). We also characterized the exciton generation zone in the EML with versatile experimental and theoretical evidences. In addition, the investigated hybrid WOLED based on TADF emitter exhibited 2 times enhanced device lifetime compared to the device without mixed host system.

These results give a starting point for further research toward high-performance and stable hybrid WOLEDs.

Bibilography

[1] M. Pope, H. P. Kallmann, and P. Magnante, "Electroluminescence in Organic Crystals", *The Journal of Chemical Physics* **38**, 2042 (1963).

[2] N. Vityuk and V. Mikho, "ELECTROLUMINESCENCE OF ANTHRACENE EXCITED BY PI-SHAPED VOLTAGE PULSES", *SOVIET PHYSICS SEMICONDUCTORS-USSR* **6**, 1497 (1973).

[3] P. S. Vincett, W. A. Barlow, R. A. Hann, and G. G. Roberts, "Electrical conduction and low voltage blue electroluminescence in vacuum-deposited organic films", *Thin Solid Films* **94**, 171 (1982).

[4] R. H. Partridge, "Electroluminescence from polyvinylcarbazole films: 3. Electroluminescent devices", *Polymer* **24**, 748 (1983).

[5] C. W. Tang and S. A. VanSlyke, "Organic electroluminescent diodes", *Applied Physics Letters* **51**, 913 (1987).

[6] C. W. Tang, S. A. VanSlyke, and C. H. Chen, "Electroluminescence of doped organic thin films", *Journal of Applied Physics* **65**, 3610 (1989).

[7] J. H. Burroughes, D. D. C. Bradley, A. R. Brown, R. N. Marks, K. Mackay, R. H. Friend, P. L. Burns, and A. B. Holmes, "Light-emitting diodes based on conjugated polymers", *Nature* **347**, 539 (1990).

[8] J. Kido, K. Hongawa, K. Okuyama, and K. Nagai, "White light-emitting organic electroluminescent devices using the poly(N-vinylcarbazole) emitter layer doped with three fluorescent dyes", *Applied Physics Letters* **64**, 815 (1994).

[9] M. A. Baldo, D. F. O'Brien, Y. You, A. Shoustikov, S. Sibley, M. E. Thompson, and S. R. Forrest, "Highly efficient phosphorescent emission from organic electroluminescent devices", *Nature* **395**, 151 (1998).

[10] J. Kido, T. Matsumoto, T. Nakada, J. Endo, K. Mori, N. Kawamura, and A. Yokoi, "27.1: Invited Paper: High Efficiency Organic EL Devices having Charge Generation Layers", *SID Symposium Digest of Technical Papers* **34**, 964 (2003).

[11] K. Walzer, B. Maennig, M. Pfeiffer, and K. Leo, "Highly Efficient Organic Devices Based on Electrically Doped Transport Layers", *Chemical Reviews* **107**, 1233 (2007).

[12] S. Möller and S. R. Forrest, "Improved light out-coupling in organic light emitting diodes employing ordered microlens arrays", *Journal of Applied Physics* **91**, 3324 (2002).

[13] B. W. D'Andrade and J. J. Brown, "Organic light-emitting device luminaire for illumination applications", *Applied Physics Letters* **88**, 192908 (2006).

[14] Y. Sun and S. R. Forrest, "Enhanced light out-coupling of organic light-emitting devices using embedded low-index grids", *Nat Photon* **2**, 483 (2008).

[15] N. Nakamura, N. Fukumoto, F. Sinapi, N. Wada, Y. Aoki, and K. Maeda, "40.4: Glass Substrates for OLED Lighting with High Out-Coupling Efficiency", *SID Symposium Digest of Technical Papers* **40**, 603 (2009).

[16] S. Reineke, F. Lindner, G. Schwartz, N. Seidler, K. Walzer, B. Lussem, and K. Leo, "White organic light-emitting diodes with fluorescent tube efficiency", *Nature* **459**, 234 (2009).

[17] Idemitsu Kosan, http://www.idemitsu.com/products/electronic/el/performance.html (2011)

[18] Universal Display, http://www.oled.com/default.asp?contentID=604 (2012)

[19] N. Ide, T. Komoda, and J. Kido, "Organic light-emitting diode (OLED) and its application to lighting devices", *SPIE Proceedings* **6333**, 63330M (2006).

[20] LG Display, http://www.lgoledlight.com/index.do (2016)

[21] R. H. Jordan, A. Dodabalapur, M. Strukelj, and T. M. Miller, "White organic electroluminescence devices", *Applied Physics Letters* **68**, 1192 (1996).

[22] R. S. Deshpande, V. Bulović, and S. R. Forrest, "White-light-emitting organic electroluminescent devices based on interlayer sequential energy transfer", *Applied Physics Letters* **75**, 888 (1999).

[23] S. Liu, J. Huang, Z. Xie, Y. Wang, and B. Chen, "Organic white light electroluminescent devices", *Thin Solid Films* **363**, 294 (2000).

[24] C. W. Ko and Y. T. Tao, "Bright white organic light-emitting diode", *Applied Physics Letters* **79**, 4234 (2001).

[25] Z.-l. Zhang, X.-y. Jiang, W.-q. Zhu, B.-x. Zhang, and S.-h. Xu, "A white organic light emitting diode with improved stability", *Journal of Physics D: Applied Physics* **34**, 3083 (2001).

[26] S. Tokito, T. Iijima, T. Tsuzuki, and F. Sato, "High-efficiency white phosphorescent organic light-emitting devices with greenish-blue and red-emitting layers", *Applied Physics Letters* **83**, 2459 (2003).

[27] B. W. D'Andrade, R. J. Holmes, and S. R. Forrest, "Efficient Organic Electrophosphorescent White-Light-Emitting Device with a Triple Doped Emissive Layer", *Advanced Materials* **16**, 624 (2004).

[28] Universal Display, http://www.printedelectronicsworld.com/articles/european_projects_accelerate_oled_technology_for_mainstream_lighting_00000972.asp (2004)

[29] General Electrics, http://www.ge.com/de/ourcompany/focus/focus/06.html (2004)

[30] Universal Display, http://www.ledsmagazine.com/news/2/8/5/1 (2005)

[31] J. Kido, http://www.sciencemag.org/cgi/content/full/310/5755/1762 (2005)

[32] Philips and Novaled, http://ledsmagazine.com/news/2/5/28 (2005)

[33] Konika Minolta, http://www.konicaminolta.com/about/research/oled/advanced/vol01.html (2006)

[34] Philips and Novaled, http://www.ledsmagazine.com/news/3/6/8/1 (2006)

[35] Y. Sun, N. C. Giebink, H. Kanno, B. Ma, M. E. Thompson, and S. R. Forrest, "Management of singlet and triplet excitons for efficient white organic light-emitting devices", *Nature* **440**, 908 (2006).

[36] Universal Display, http://www.printedelectronicsworld.com/articles/european_projects_accelerate_oled_technology_for_mainstream_lighting_00000972.asp (2007)

[37] Y. Sun and S. R. Forrest, "High-efficiency white organic light emitting devices with three separate phosphorescent emission layers", *Applied Physics Letters* **91**, 263503 (2007).

[38] Universal Display, http://www.oled-info.com/lg/udc_white_oled_technology_exceeds_100_lm_w (2008)

[39] Philips and Novaled, http://www.hitechprojects.com/euprojects/olla/news/press_release_june_2008/OLLA_pressrelease6_v4.pdf (2008)

[40] M. C. Gather, A. Köhnen, and K. Meerholz, "White Organic Light-Emitting Diodes", *Advanced Materials* **23**, 233 (2011).

[41] K. Yamae, H. Tsuji, V. Kittichungchit, N. Ide, and T. Komoda, "66.2: Invited Paper: Highly Efficient White OLEDs with over 100 lm/W for General Lighting", *SID Symposium Digest of Technical Papers* **44**, 916 (2013).

[42] Konica Minolta, http://www.oled-info.com/konica-minolta-developed-worlds-most-efficient-oled-panel-131-lmw (2014)

[43] J. Liu, Q. G. Zhou, Y. X. Cheng, Y. H. Geng, L. X. Wang, D. G. Ma, X. B. Jing, and F. S. Wang, "The First Single Polymer with Simultaneous Blue, Green, and Red Emission for White Electroluminescence", *Advanced Materials* **17**, 2974 (2005).

[44] J. Liu, C. Min, Q. Zhou, Y. Cheng, L. Wang, D. Ma, X. Jing, and F. Wang, "Blue light-emitting polymer with polyfluorene as the host and highly fluorescent 4-dimethylamino-1,8-naphthalimide as the dopant in the sidechain", *Applied Physics Letters* **88**, 083505 (2006).

[45] J. Kido, M. Kimura, and K. Nagai, "Multilayer White Light-Emitting Organic Electroluminescent Device", *Science* **267**, 1332 (1995).

[46] J. Kido, "61.1: Invited Paper: High Performance OLEDs for Displays and General Lighting", *SID Symposium Digest of Technical Papers* **39**, 931 (2008).

[47] T.-W. Lee, T. Noh, B.-K. Choi, M.-S. Kim, D. W. Shin, and J. Kido, "High-efficiency stacked white organic light-emitting diodes", *Applied Physics Letters* **92**, 043301 (2008).

[48] R. J. Holmes, B. W. D'Andrade, S. R. Forrest, X. Ren, J. Li, and M. E. Thompson, "Efficient, deep-blue organic electrophosphorescence by guest charge trapping", *Applied Physics Letters* **83**, 3818 (2003).

[49] C. L. Mulder, K. Celebi, K. M. Milaninia, and M. A. Baldo, "Saturated and efficient blue phosphorescent organic light emitting devices with Lambertian angular emission", *Applied Physics Letters* **90**, 211109 (2007).

[50] G. Schwartz, S. Reineke, T. C. Rosenow, K. Walzer, and K. Leo, "Triplet Harvesting in Hybrid White Organic Light-Emitting Diodes", *Advanced Functional Materials* **19**, 1319 (2009).

[51] N. Sun, Q. Wang, Y. Zhao, Y. Chen, D. Yang, F. Zhao, J. Chen, and D. Ma, "High-Performance Hybrid White Organic Light-Emitting Devices without Interlayer between Fluorescent and Phosphorescent Emissive Regions", *Advanced Materials* **26**, 1617 (2014).

[52] M. A. Baldo, C. Adachi, and S. R. Forrest, "Transient analysis of organic electrophosphorescence. II. Transient analysis of triplet-triplet annihilation", *Physical Review B* **62**, 10967 (2000).

[53] J. Ye, Z. Chen, F. An, M. Sun, H.-W. Mo, X. Zhang, and C.-S. Lee, "Achieving Highly Efficient Simple-Emission Layer Fluorescence/Phosphorescence Hybrid White Organic Light-Emitting Devices via Effective Confinement of Triplets", *ACS Applied Materials & Interfaces* **6**, 8964 (2014).

[54] J. Ye, C.-J. Zheng, X.-M. Ou, X.-H. Zhang, M.-K. Fung, and C.-S. Lee, "Management of Singlet and Triplet Excitons in a Single Emission Layer: A Simple Approach for a High-Efficiency Fluorescence/Phosphorescence Hybrid White Organic Light-Emitting Device", *Advanced Materials* **24**, 3410 (2012).

[55] Y. Divayana, S. Liu, A. K. K. Kyaw, and X. W. Sun, "Efficient extraction of singlet–triplet excitons for high-efficient white organic light-emitting diode with a multilayer emission region", *Organic Electronics* **12**, 1 (2011).

[56] X.-K. Liu, C.-J. Zheng, M.-F. Lo, J. Xiao, Z. Chen, C.-L. Liu, C.-S. Lee, M.-K. Fung, and X.-H. Zhang, "Novel Blue Fluorophor with High Triplet Energy Level for High Performance Single-Emitting-Layer Fluorescence and Phosphorescence Hybrid White Organic Light-Emitting Diodes", *Chemistry of Materials* **25**, 4454 (2013).

[57] Y. Chen, F. Zhao, Y. Zhao, J. Chen, and D. Ma, "Ultra-simple hybrid white organic light-emitting diodes with high efficiency and CRI trade-off: Fabrication and emission-mechanism analysis", *Organic Electronics* **13**, 2807 (2012).

[58] F. Zhao, Z. Zhang, Y. Liu, Y. Dai, J. Chen, and D. Ma, "A hybrid white organic light-emitting diode with stable color and reduced efficiency roll-off by using a bipolar charge carrier switch", *Organic Electronics* **13**, 1049 (2012).

[59] H. Uoyama, K. Goushi, K. Shizu, H. Nomura, and C. Adachi, "Highly efficient organic light-emitting diodes from delayed fluorescence", *Nature* **492**, 234 (2012).

[60] F. B. Dias, K. N. Bourdakos, V. Jankus, K. C. Moss, K. T. Kamtekar, V. Bhalla, J. Santos, M. R. Bryce, and A. P. Monkman, "Triplet Harvesting with 100% Efficiency by Way of Thermally Activated Delayed Fluorescence in Charge Transfer OLED Emitters", *Advanced Materials* **25**, 3707 (2013).

[61] M. P. Gaj, C. Fuentes-Hernandez, Y. Zhang, S. R. Marder, and B. Kippelen, "Highly efficient Organic Light-Emitting Diodes from thermally activated

delayed fluorescence using a sulfone–carbazole host material", *Organic Electronics* **16**, 109 (2015).

[62] A. Endo, M. Ogasawara, A. Takahashi, D. Yokoyama, Y. Kato, and C. Adachi, "Thermally Activated Delayed Fluorescence from Sn4+–Porphyrin Complexes and Their Application to Organic Light Emitting Diodes — A Novel Mechanism for Electroluminescence", *Advanced Materials* **21**, 4802 (2009).

[63] J. C. Deaton, S. C. Switalski, D. Y. Kondakov, R. H. Young, T. D. Pawlik, D. J. Giesen, S. B. Harkins, A. J. M. Miller, S. F. Mickenberg, and J. C. Peters, "E-Type Delayed Fluorescence of a Phosphine-Supported Cu2(μ-NAr2)2 Diamond Core: Harvesting Singlet and Triplet Excitons in OLEDs", *Journal of the American Chemical Society* **132**, 9499 (2010).

[64] A. Endo, K. Sato, K. Yoshimura, T. Kai, A. Kawada, H. Miyazaki, and C. Adachi, "Efficient up-conversion of triplet excitons into a singlet state and its application for organic light emitting diodes", *Applied Physics Letters* **98**, 083302 (2011).

[65] J. W. Sun, J.-H. Lee, C.-K. Moon, K.-H. Kim, H. Shin, and J.-J. Kim, "A Fluorescent Organic Light-Emitting Diode with 30% External Quantum Efficiency", *Advanced Materials* **26**, 5684 (2014).

[66] D. R. Lee, B. S. Kim, C. W. Lee, Y. Im, K. S. Yook, S.-H. Hwang, and J. Y. Lee, "Above 30% External Quantum Efficiency in Green Delayed Fluorescent Organic Light-Emitting Diodes", *ACS Applied Materials & Interfaces* **7**, 9625 (2015).

[67] H. Nakanotani, K. Masui, J. Nishide, T. Shibata, and C. Adachi, "Promising operational stability of high-efficiency organic light-emitting diodes based

on thermally activated delayed fluorescence", *Scientific Reports* **3**, 2127 (2013).

[68] Y. J. Cho, K. S. Yook, and J. Y. Lee, "A Universal Host Material for High External Quantum Efficiency Close to 25% and Long Lifetime in Green Fluorescent and Phosphorescent OLEDs", *Advanced Materials* **26**, 4050 (2014).

[69] Q. Zhang, B. Li, S. Huang, H. Nomura, H. Tanaka, and C. Adachi, "Efficient blue organic light-emitting diodes employing thermally activated delayed fluorescence", *Nat Photon* **8**, 326 (2014).

[70] A. S. D. Sandanayaka, T. Matsushima, and C. Adachi, "Degradation Mechanisms of Organic Light-Emitting Diodes Based on Thermally Activated Delayed Fluorescence Molecules", *The Journal of Physical Chemistry C* **119**, 23845 (2015).

[71] Q. Zhang, D. Tsang, H. Kuwabara, Y. Hatae, B. Li, T. Takahashi, S. Y. Lee, T. Yasuda, and C. Adachi, "Nearly 100% Internal Quantum Efficiency in Undoped Electroluminescent Devices Employing Pure Organic Emitters", *Advanced Materials* **27**, 2096 (2015).

[72] B. Liu, D. Luo, J. Zou, D. Gao, H. Ning, L. Wang, J. Peng, and Y. Cao, "A host-guest system comprising high guest concentration to achieve simplified and high-performance hybrid white organic light-emitting diodes", *Journal of Materials Chemistry C* **3**, 6359 (2015).

[73] Y. J. Cho, K. S. Yook, and J. Y. Lee, "Cool and warm hybrid white organic light-emitting diode with blue delayed fluorescent emitter both as blue emitter and triplet host", *Scientific Reports* **5**, 7859 (2015).

[74] X.-K. Liu, Z. Chen, J. Qing, W.-J. Zhang, B. Wu, H. L. Tam, F. Zhu, X.-H. Zhang, and C.-S. Lee, "Remanagement of Singlet and Triplet Excitons in

Single-Emissive-Layer Hybrid White Organic Light-Emitting Devices Using Thermally Activated Delayed Fluorescent Blue Exciplex", *Advanced Materials* **27**, 7079 (2015).

[75] D. Zhang, L. Duan, Y. Zhang, M. Cai, D. Zhang, and Y. Qiu, "Highly efficient hybrid warm white organic light-emitting diodes using a blue thermally activated delayed fluorescence emitter: exploiting the external heavy-atom effect", *Light Sci Appl* **4**, e232 (2015).

[76] Z. Wu, J. Luo, N. Sun, L. Zhu, H. Sun, L. Yu, D. Yang, X. Qiao, J. Chen, and C. Yang, "High-Performance Hybrid White Organic Light-Emitting Diodes with Superior Efficiency/Color Rendering Index/Color Stability and Low Efficiency Roll-Off Based on a Blue Thermally Activated Delayed Fluorescent Emitter", *Advanced Functional Materials* (2016).

[77] H. Sasabe, J.-i. Takamatsu, T. Motoyama, S. Watanabe, G. Wagenblast, N. Langer, O. Molt, E. Fuchs, C. Lennartz, and J. Kido, "High-Efficiency Blue and White Organic Light-Emitting Devices Incorporating a Blue Iridium Carbene Complex", *Advanced Materials* **22**, 5003 (2010).

[78] Q. Wang, J. Ding, D. Ma, Y. Cheng, L. Wang, X. Jing, and F. Wang, "Harvesting Excitons Via Two Parallel Channels for Efficient White Organic LEDs with Nearly 100% Internal Quantum Efficiency: Fabrication and Emission-Mechanism Analysis", *Advanced Functional Materials* **19**, 84 (2009).

[79] L. Zhu, Z. Wu, J. Chen, and D. Ma, "Reduced efficiency roll-off in all-phosphorescent white organic light-emitting diodes with an external quantum efficiency of over 20%", *Journal of Materials Chemistry C* **3**, 3304 (2015).

[80] N. Sun, Q. Wang, Y. Zhao, D. Yang, F. Zhao, J. Chen, and D. Ma, "A hybrid white organic light-emitting diode with above 20% external quantum efficiency and extremely low efficiency roll-off", *Journal of Materials Chemistry C* **2**, 7494 (2014).

[81] C. Adachi, M. A. Baldo, M. E. Thompson, and S. R. Forrest, "Nearly 100% internal phosphorescence efficiency in an organic light-emitting device", *Journal of Applied Physics* **90**, 5048 (2001).

[82] Cynora, https://awesomedisplay.wordpress.com/2016/10/06/cynora-latest-tadf-blue-emitters-feature-higher-efficiency-and-lifetime/ (2016)

Publication

[1] SCI Journal Papers

1. **Yongwon Kwon**, Yongnam Kim, Hyunkoo Lee, Changhee Lee, and Jeonghun Kwak, “Composite film of poly(3,4-ethylenedioxythiophene):poly(styrenesulfonate) and MoO3 as an efficient hole injection layer for polymer light-emitting diodes”, *Organic Electronics* **15**, 1083 (2014).
2. Hyung-Jun Song, Jun Young Kim, **Yongwon Kwon**, Youngjun Ko, Donggu Lee, Ho Jung Syn, Jiyun Song, Jeonghun Kwak, and Changhee Lee, “Improvement in the efficiency of organic solar cells using a low-temperature evaporable optical spacer”, *Japanese Journal of Applied Physics* **53**, 08NJ04 (2014).
3. Hyunkoo Lee, **Yongwon Kwon**, Heeyoung Jung, Jeong-Ik Lee, and Changhee Lee, “Enhanced performances in inverted bottom-emission organic light-emitting diodes with KBH4-doped electron-injection layer”, **Physica Status Solidi A 211**, 1807 (2014).
4. Woo-Young Park, **Yongwon Kwon**, Changhee Lee, and Ki-Woong Whang, “Light outcoupling enhancement from top-emitting organic light-emitting

diodes made on a nano-sized stochastic texture surface", *Optics Express* **22**, A1687 (2014).

5. Woo-Yong Park, **Yongwon Kwon**, Hee-Woon Cheong, Changhee Lee, and Ki-Woong Whang, "Increased light extraction efficiency from top-emitting organic light-emitting diodes employing a mask-free plasma-etched stochastic polymer surface", *Journal of Applied Physics* **119**, 95502 (2016).
6. Jiyun Song, Hyung-Jun Song, Jun Young Kim, Yeonkyung Lee, Myeongjin Park, **Yongwon Kwon**, Youngjun Ko, and Changhee Lee, "Improvement in the Photocurrent of Inverted Organic Solar Cells Using MoOx-Doped TAPC as a p-Type Optical Spacer", *Journal of Nanoscience and Nanotechnology* **16**, 5008 (2016).

[2] SCIE Journal Papers

1. Hyunkoo Lee, **Yongwon Kwon**, Changhee Lee, "Improved performances in organic and polymer light-emitting diodes using solution-processed vanadium pentoxide as a hole injection layer", *Journal of the Society for Information Display* **20**, 640 (2012).

2. Jongseok Han, Donghyun Ko, Myeongjin Park, Jeongkyun Roh, Heeyoung Jung, Yeonkyung Lee, **Yongwon Kwon**, Jiho Sohn, Wan Ki Bae, Byung Doo Chin, and Changhee Lee, "Toward high-resolution, inkjet-printed, quantum dot light-emitting diodes for next-generation displays", *Journal of the Society for Information Display* **24**, 545 (2016).

[3] International Conferences

1. **Yongwon Kwon**, Minsun Yoo, Hyunkoo Lee, Jungjin Yang, and Changhee Lee, "P-doped Di-[4-(N,N-ditolyl-amino)-phenyl]cyclohexane for Improving Power Efficiency of Organic Light-Emitting Diodes", *The 51st SID International Symposium, Seminar & Exhibition*, May 2013.
2. **Yongwon Kwon**, Jongseok Han, and Changhee Lee, "Improved Electron Injection in Organic Light-Emitting Diodes Using Samarium Doped Electron Transport Layer", *The 52nd SID International Symposium, Seminar & Exhibition*, Jun 2014.
3. **Yongwon Kwon**, Yongnam Kim, Jeonghun Kwak, and Changhee Lee, "Enhanced Stability of Polymer Light-Emitting Diodes using Mixture of Poly(3,4-ethylenedioxythiophene):poly(styrenesulfonate) and MoO_3", *The 14th International Meeting on Information Display*, August 2014.
4. **Yongwon Kown**, Jiho Sohn, Jeonghun Kwak, and Changhee Lee, "Efficient Electron Injecting Semi-Transparent Cathodes Using Samarium and Silver for Transparent Organic Light-Emitting Diodes", *International Symposium on Flexible Organic Electronics*, July 2015.
5. **Yongwon Kwon**, Jiho Sohn, and Changhee Lee, "Wide Color Gamut Top-Emitting White Organic Light-Emitting Diodes for High Quality Display Application", *The 15th International Meeting on Information Display*, August 2015.
6. **Yongwon Kwon**, Jiho Sohn, and Changhee Lee, "Efficient Triplet Harvesting in White Organic Light-Emitting Diodes with Non-Doped Blue Emitter", *The 16th International Meeting on Information Display*, **Best Poster Award**, August 2016

한글 초록

본 논문에서는 혼합물 호스트 발광층을 사용한 고효율 백색 하이브리드 유기발광다이오드 소자의 설계 전략 및 열활성 지연형광 물질을 사용한 청색 유기발광다이오드 소자의 수명 향상 효과를 연구하였다. 먼저, 일반적인 형광 청색 발광물질을 사용하여 중간층을 사용하지 않는 고효율 하이브리드 백색 유기발광다이오드의 개발을 수행하였고, 본 소자에서는 형광 청색 발광층과 인광 황색 발광층 사이의 엑시톤 분포 조절을 위한 혼합물 호스트를 청색 발광층에 적용하였다. 개발된 소자는 중간층을 사용한 백색 소자 대비 향상된 전계발광 특성을 보였지만 상대적으로 나쁜 수명 특성을 보였으며, 이는 청색 형광 발광층과 황색 인광 발광층의 직접접합에 의한 엑시톤 퀜칭에 의한 것으로 판단된다. 이러한 결과를 통하여 일반적 형광 청색 발광물질의 낮은 삼중항 에너지 준위가 가진 문제를 해소하는 것이 필요하다고 판단되며 높은 삼중항 에너지 준위를 가지는 열활성 지연형광 특성의 청색 발광물질을 도입하였다.

다음으로, 열활성 지연형광 청색 발광물질 기반 유기발광다이오드 소자의 열화 메커니즘을 규명하고, 소자 수명 향상을 위하여 혼합물 호스트를 적용하는 연구를 수행하였다. 열활성 지연형광 물질 기반 유기발광다이오드의 주요 열화 원인은 발광층 호스트 물질의 불안정성 때문이며, 장기간 열화의 경우 물질의 전기화학적 불안정성에 의하여 발생함을 규명하였다. 또한 소자 열화에 의한 생성물이 엑시톤 퀜처로

작용함을 확인하였으며, 본 연구에서 적용된 혼합물 호스트는 명백히 발광층의 활성준위 스트레스에 대한 안정성을 향상시켜 소자 수명향상에 기여함을 확인하였다.

마지막으로 앞서 확인된 혼합물 호스트가 적용된 열활성 지연형광 청색 발광층을 사용하여 고효율, 뛰어난 색안정성, 적은 효율 감퇴, 소자 안정성을 가진 하이브리드 백색 유기발광다이오드 소자를 개발하였다. 개발된 소자는 최대 22.1 %, 59.3 cd/A, 50.3 lm/W 의 외부양자효율, 전류효율, 및 전력효율을 보였으며, 아주 적은 색좌표 변화 < (0.003, 0.003)를 보였다. 또한 다양한 실험을 통하여 소자 내부의 엑시톤 형성 영역을 특정 지었다. 덧붙여 개발된 소자는 혼합물 호스트를 사용하지 않은 소자 대비 2 배 향상된 소자 수명을 보였다.

결론적으로, 혼합물 호스트는 고성능 하이브리드 백색 유기발광다이오드 소자에 쉽게 적용될 수 있으며, 효과적으로 엑시톤 형성 영역을 넓히며 발광층의 활성준위 스트레스에 대한 안정성을 향상시킴을 알 수 있다. 본 논문에서 연구된 메커니즘과 소자 개발 과정은 향후 고효율 장수명 하이브리드 백색 유기발광다이오드의 개발에 기여하는 출발점이 될 수 있을 것으로 예상한다.

주요어: 유기발광다이오드, 하이브리드 백색, 열활성 지연형광, 수명

학번: 2013-30219